A Pilot Field Implementation of Suction Dredging for Sustainable Sediment Management of Dam Reservoirs

Sameh A. Kantoush[1*], Ahmad Mousa[2*], Ebi Meshkati Shahmirzadi[3], Temmyo Toshiyuki[4], Tetsuya Sumi[5]

[1]Associate Professor, Disaster Prevention Research Institute, Kyoto University
Email: kantoush.samehahmed.2n@kyoto-u.ac.jp

[2]Senior Lecturer, School of Engineering, Monash University Malaysia
Email: ahmad.mousa@monash.edu

[3]PhD, Researcher, Deltares, Delft, The Netherlands
Email: ebi.meshkatishahmirzadi@deltares.nl

[4]Engineer, Hazama Ando Corporation
Email: temmyo.toshiyuki@ad-hzm.co.jp

[5]Professor, Disaster Prevention Research Institute, Kyoto University
Email: sumi.tetsuya.2s@kyoto-u.ac.jp

[*]Corresponding Authors

Abstract

The buildup of sediment deposits in reservoirs is a longstanding problem with serious consequences on their functionality and the eco-environment of their river systems. In the last two decades, hydraulic dredging has been opted for as a more viable engineering solution to restore reservoirs' sustainability. This study proposes a novel ejector-pump dredging system (EPDS) that solely utilizes hydro-dredging for removal and transport of the sediments deposited at the reservoir's bed. Unlike conventional dredging methods, air is injected into the header pipeline to create a turbulent three-phase flow regime that enhances solid's suspension and continuous flow in the system. Introducing air effectively reduces the critical value of the deposition velocity of the dredged solids and transport them in a slug flow regime. This technique minimizes the tendency of the sediment to settle and, therefore, eliminates system plugging. A laboratory prototype of the proposed system has proven the efficacy of removal and transport of mixed-size sediments up to 150 mm. Field trials have further shown the feasibility of the proposed system. Removal of large sediments with productivity approaching 70 m^3/h was made possible using the suction-type EPDS. The hopper-type EPDS enabled carrying the dredged material for up to 1,000 m without resorting to a booster pump. The developed system was successfully used as part of an integrated dredging management program carried out for the Oouchibaru, Saigo, and Yamasubaru dams in the Mimi River Basin, Japan. The very low turbidity levels recorded during the sediment dredging and transport operations of EPDS are indicative of the eco-friendly performance of the system.

Keywords: Sediment management; suction dredging; dam reservoir; three-phase flow; ejector-pump dredging system, turbidity control

Introduction

Sediment management in dam reservoirs has become an increasingly inevitable priority for management boards of river basins worldwide. The recurrence of excessive siltation upstream of dam reservoirs not only leads to a costly reservoir storage maintenance, but also imbalances the sediment inflow and outflow in the reservoirs which may cause dire consequences on rivers' ecosystem (Morris, 2020; Kantoush and Sumi, 2019). A range of sediment management techniques, such as flushing, sediment bypass tunnel, sluicing and dredging, has been developed to restore dams' functionality and recover their ecosystem (Auel et al., 2016). Selecting one or a combination of these techniques is site-specific and mainly depends on the turnover rate of both water and sediments (Kantoush and Sumi, 2016). The factors governing the selection include the type and amount of sediments, dredging depth, distance to the disposal site, and operating conditions (Chaudhuri et al., 2020; Bray et al., 1996).

Hydraulic dredgers utilize water to break and lift the sediments and transport them to a designated disposal site (Turner, 1996; Herbich, 2000). They are capable of removing a wide array of materials, e.g., clay, mud, silt, sand, gravel and reef material (Morris, 2020; Lewis and Randall, 2015). Hydraulic dredgers include trailing suction hopper (TSHD), bucket wheel, plain suction/dustpan, and cutter-suction head (CSD). Siphon dredging and sediment evacuation pipeline system are differentiated from other hydraulic dredger by the absence of a pump, and a continuously submerged discharge (Morris, 2020). Conventional hydraulic dredging systems have limited transportation lengths and require large powers to restore the storage capacity of a reservoir (Bruk, 1985). They are typically challenged by the frequent deposition of the dredged material in transport pipeline, especially for long distances. This could lead to serious subsequent problems, such as excessive pressure drops, equipment failure, and pipeline erosion, all of which adversely affect dredging productivity (Chaudhuri et al., 2020).

The presence of two or three phases (water, sediments and air) in a transport pipeline can form different slurry flow regimes (Herbich, 2000): homogeneous, heterogeneous, moving bed, and stationary bed. Mandhane et al. (1974) conducted two-phase air and water flow tests to monitor the flow regimes of water-air mixtures in a horizontal pipe. They found that the flow-patterns depend largely on the influx combinations of water and air. In terms of pattern, there are six key flow regimes, namely, dispersed bubble, annular, elongated bubble, slug, stratified, and stratified wavy flow (Taitel and Dukler, 1976). Three-phase flows (air-water-sand) in horizontal pipe has been closely investigated in both experimental and numerical studies using different air concentrations (e.g. Goharzadeh et al., 2010; Dabirian et al., 2016a and 2016b; Leporini et al., 2018). The existing studies are mainly devoted to applications in petroleum industry at laboratory scale. This study, in contrary, investigates the multi-phase flow sediment transport tailored to dredging application at both laboratory and commercial scale, with a focus on impact of air injection on the efficiency of dredging system as a whole. This study was motivated by the growing demand for dredging to restore the storage capacity of several dam reservoirs in Japan. The restoration requirements span efficient, economical, reliable, and environmentally accepted dredging. Reservoir dredging is being carried out for one quarter of the 3,000 dams in Japan. We proposed a novel hydro-suction dredging technique that chiefly employs suction for sediment removal. The air injection creates a multiphase flow (water-air-solid) that can optimize the suction power and equally minimize plugging in the transportation components. The adopted concept has proven to be successful both at the laboratory scale and in the field trials in Morotsuka, Yamasubaru, Saigo, and Ouchibaru reservoirs in Japan. The implementation includes sediment relocation within the reservoirs as well as transporting the removed dredged sediment to designated disposal areas.

Laboratory Prototype

A laboratory prototype utilizing forced hydro-suction for sediment removal was built as a proof of the concept. Experimental evaluation of the system establishes a fundamental understanding of the system's performance and examines its sensitivity to the design parameters. The mechanism and efficiency of the sediment suction and transport were closely monitored for system optimization.

Operating Concept

The proposed ejector-pump dredging system (EPDS) employs a high-pressure water jet applied through a nozzle to create a negative pressure in the ejector house. The ejector, subsequently, delivers the necessary energy to draw the sediment from the reservoir bed through a vertical suction pipeline (**Fig. 1**). The sediments entering the ejector house are pushed into the transport pipeline under the high-pressure water jet. The ejector-pump has two specific characteristics: a controlled air inlet into the pump; the unthrottled inner straight pipe (**Fig. 1**). This configuration minimizes cavitation and abrasion of the pump. By changing a combination of diameters of the nozzle and the inner pipe, the suction flow rate can be adjusted. Another advantage is that the jet flow washes the sediment while passing through the ejector-pump. Since the new pump does not have rotary parts (impeller wheel), it is structurally simple and easy to maintain.

As schematically shown in **Fig. 2**, the experimental setup consists of three major sections, namely, the initial driving force, suction, and transport. The driving force section comprises a high-pressure pump connected to a storage tank. This component of the setup generates a high velocity water jets responsible for creating a negative pressure (suction) in the ejector. Suction from the sediments tank is furnished via a vertical pipeline having an internal diameter (D_{sp}). Several pipe lengths (H_{suc}) were considered in this setup (**Table 1**). Transport

of the drawn sediments was made possible through a horizontal pipeline (L_{tp}, D_{tp}) running from the air compressor injection point to the downstream end (disposal). The compressor injects a controlled air concentration at the head of the transport pipeline. A one-meter segment of the horizontal transport pipe was made of transparent plexiglass to permit flow visualization using the large-scale particle image velocimetry (LSPIV) technique. The system is equipped with two static-dynamic pressure gauges ($P1$ and $P2$) at the high-pressure pump and the downstream of the ejector house, respectively. Three pressure probes/piezometers ($P3$, $P4$ and $P5$, located 3.5 m apart) are used to measure pressure differential in the transport pipeline. To this end, the designed experimental program aims to utilize the collected observations to identify the key factors and parameters that control suction dredging. Subsequently, the system was optimized to enhance efficiency and minimize clogging potential.

Design Parameters

The suction power (Q_{suc}) from a sediment tank is defined as the volume of water and sediment lifted during a specific time period. Several inherent properties of the flow mix, namely, the densities of water (ρ_w) and sediments (ρ_s), and the grain size (d_s) affect the suction power. It is also governed by other parameters including, the pump discharge pressure (P_{pump}), air concentration (Q_{air}) injected to the pipeline, length of the suction pipeline (L_{SP}), length of the transport pipeline (L_{tp}), height of the suction pipeline (H_{sp}), diameter of the suction pipeline (D_{sp}), and diameter of the transport pipeline (D_{tp}). As such, the suction flow can be expressed as a function of these parameters:

$$Q_{suc} = f(d_s, P_{pump}, Q_{air}, L_{tp}, H_{sp}, D_{sp}, D_{tp}, \rho_w, \rho_s) \quad (1)$$

The experiments were carried out for five sediment grain sizes, five pump discharges, eight air concentration levels, four lengths of suction pipe, seven lengths of transportation pipeline and five suction heads. The laboratory program amounts to a total of 215 experiments,

as summarized in **Table 1**. Two liters of sediments (V_s) was placed in the sediment storage tank. The time needed for suction and removal of the sediments at the end of the transport pipe was recorded (t_{ws}) for each test. Thus, the sediment discharge rate (Q_s) can be calculated as:

$$Q_s = \frac{V_s}{t_{ws}} \tag{2}$$

The difference between the water level in the sediment tank before and after the test yields the released volume of water and sediments (V_{ws}). The suction power (Q_{suc}) can be accordingly estimated as:

$$Q_{suc} = \frac{V_{ws}}{t_{ws}} \tag{3}$$

The superficial velocities J_A and J_W are respectively defined as the air concentration (Q_{air}) and water-sediment flow discharge (Q_{ws}) passing through the pipeline cross-sectional area (A_p). Q_{ws} in the pipeline is the sum of the pump discharge (Q_{pump}) and the water-sediment sucked from the sediment reservoir (Q_{suc}). The superficial velocities of the flow in the pipeline can be subsequently expressed as follows:

$$J_A = \frac{Q_{air}}{A_p} \quad \textit{(air)} \tag{4}$$

$$J_W = \frac{Q_{W-total}}{A_p} \quad \textit{(water-sediment)} \tag{5}$$

$$J = J_A + J_W \quad \textit{(total)} \tag{6}$$

The overall efficiency (E_{EPDS}) of the system performance can be defined as the ratio between the sediment and the pump discharges:

$$E_{EPDS} = \frac{Q_s}{Q_{pump}} \tag{7}$$

Both Q_{suc} and E_{EPDS} are practical indicators of the performance. They can subsequently provide a reasonable guidance for system design and optimization. However, they are likely to be influenced by sediment size (d_s), geometry of the prototype (D_{sp}, D_{tp}, L_{sp},

158 L_{tp}), and the hydraulic parameters (Q_{air}, H_{suc}). Sediment removal concentrations in suction
159 pipeline (C_{ss}) and transport (C_{st}) phases are respectively expressed as follows:

160 $$C_{ss} = \frac{Q_s}{(Q_s+Q_w)} \times 100 \quad (8)$$

161 $$C_{st} = \frac{Q_s}{(Q_{pump}+Q_s+Q_w)} \times 100 \quad (9)$$

162 Equations 8 and 9 provide additional practical measures for the efficiency of sediment
163 removal in the suction and transport pipelines, respectively.

164 **Results**

165 The laboratory program embarks on monitoring the flow regimes using the proposed system
166 as well as evaluating the efficiency of the suction and transport phases. **Table 1** summarizes
167 the investigated ranges of the key design parameters. D_{sp} and D_{tp} were set at 25 and 36 mm,
168 respectively, for all of the presented laboratory readings. In any given trial, ρ_s, H_{suc}, L_{sp} and
169 L_{tp} were held constant unless stated otherwise. As such, the interaction between the selected
170 parameters and the laboratory measurements should not be overruled.

171 ***Flow regimes***

172 The observed air and water superficial velocities at air injections of up to 120 nl/min were as
173 follows:

174 $0.409 < J_A < 1.96$ m/sec

175 $0.411 < J_W < 1.52$ m/sec

176 The ranges for the collected velocities are overlaid on the flow-type zones depicted in
177 **Fig. S1**. The flow patterns associated with these ranges are clearly slug-plug types. When the
178 flow regime changes from elongated bubble flow to slug at the minimum superficial air
179 velocity of 0.95 m/s, the velocity at this transitions state cannot be determined with certainty.
180 Hence, the flow pattern should be closely monitored to provide a qualitative measure of the

particle movement regime. Interactions of solid-gas-liquid in a multiphase flow and flow field analysis have been investigated using the particle image velocimetry (PIV) technique (Kim et al., 2018;). In this study, large-scale particle image velocimetry (LSPIV) analysis was employed to visualize the flow pattern in the transport phase (Kantoush et al., 2011).

Fig. 3a depicts the captured flow along with the velocity distribution in TP when no air was injected into the system. This was manifested in forming a stratified flow in the pipe. Almost all velocity vectors are confined in the upper half of TP with a general horizontal flow. The flow vectors in the sediment deposits are insignificant. This indicates the inability of the stratified flow to carry the sediments. However, when 25 nl/min airflow was injected into the system, the velocity distribution has significantly changed (**Fig. 3b**). As shown by the traced trajectories, an intermittent flow pattern was observed and the velocity vectors are periodically oriented toward the bottom of TP. The efficiency of particles stirring and suspension was increased when the airflow was raised to 40 nl/min (**Fig. 3c**).

Suction phase

As discussed earlier, the applied high jet velocity drops the pressure in the ejector house and, thus, enables the system to vacuum (suck) sediments from reservoir via a suction pipeline utilizing the created pressure gradient. The wide range of discharge pump pressures (P_{pump}) and various sizes of sediments used in this study (previously reported by Meshkati Shahmirzadi et al. 2012) allowed to correlate with the suction power (Q_{suc}) at different air concentrations. At higher P_{pump}, the jet velocity of the water released from the nozzle greatly increases and causes a high pressure drop (negative pressure) in the ejector house. The created pressure gradient between the sediment tank and the ejector house subsequently lifts the water and sediments (Q_{suc}) into the EPDS header. As expected, Q_{suc} in the presence of only clear water was higher than that of the two-phase (sediment-water) flow.

Further pressure gradient can be achieved by injecting air at the downstream of the ejector house. This additional pressure differential is created between the beginning of the transport pipeline (just downstream of the ejector house) and inside of the inner pipe in the ejector house. Air injection increases the velocity of flow, i.e. J_A and J_W, and thus the velocity at the beginning of transport pipeline should be higher than that inside of the inner pipe in the ejector house. The induced dual vacuum effect enhances sediment transport with higher initial velocities compared to the zero-air injection. This reduces the risk of sediment accumulation in the beginning of pipeline and improves the efficiency of sediment transport.

The effect of the suction pipe length on flow of dredged water and sediment was tested. **Fig. 4** depicts the sediment concentration in suction pipe (C_{ss}) against Q_{suc} and Q_s for the 2 mm and 5 mm sediments. The results are shown for zero-air entrainment and pumping power (P_{pump}) of 588 kPa. Increasing the suction power Q_{suc} was associated with a linear reduction in concentration of sediment in suction pipe C_{ss}. This was observed for sediment sizes of 2 mm and 5 mm and for all lengths of the suction pipe (**Figs. 4a, b**). Moreover, for a certain C_{ss} the shorter the length of suction pipe the larger the suction power of the system $Q_{suc.}$ Having said that, this does not mean that more sediment will be removed. As can be seen in **Figs. 4c, d** there is an optimal value for C_{ss} in the shortest suction pipe (2 m) at which the maximize sediment discharge rate Q_s occurs. Thus, the maximum sediment removal performance does not occur at the highest C_{ss}. For longer suction pipes (10 and 20 m) however it was not possible to increase the C_{ss} beyond a certain concentration as the system failed at those higher concentrations. **Fig. 5** shows the maximum observed sediment discharge rate Q_s for the three suction lengths in the presence of no air injection in the transport pipe. As expected, for a certain suction pipe length, the smaller the particles are the better the performance of system regarding sediment discharge rate (Q_s) would be.

Transport phase

The differential pressure in the transport pipeline was monitored using the piezometers shown in **Fig. 2**. The pressure gradient $(\partial \mathrm{p}/\partial \mathrm{x})$ was calculated as the pressure difference between $P3$ and $P5$ divided by the distance ($\triangle$x) between piezometers:

$$\partial \mathrm{p}/\partial \mathrm{x} = \frac{P3-P5}{\triangle x} \quad (10)$$

The sediment removal in suction (C_{ss}) and the measured sediment concentration in the transport pipe (C_{st}) –**Fig. S2**– have improved by using air injection particularly for the larger sediment (5 mm). These relationship between both C_{ss} and C_{st} and the observed pressure gradient advocates that the change in the flow pattern due to air injection enhance the suction and transport processes (Meshkati Shahmirzadi et al., 2012). The relation between the length of the transport pipeline and the maximum observed sediment discharge rate (Q_s) is shown in **Fig. 6**. The maximum Q_s decreases linearly with increasing the transport length. The use of 60 nl/min air injection resulted in higher Q_s as compared to the zero-air case. The presence of air in the transportation managed to increase the sediment removal even for the near zero removal at L_{tp} of 20 m. This result suggests the need for optimizing the air concentration for long transportation, which could be extremely beneficial in the field.

System Optimization

The foregoing results provided the basis for optimization of the geometrical and hydraulic characteristics of the system. In doing so, the efficiency and the performance of the system are quantified. The concentration of the injected air is the key factor in the system optimization. Different sediment sizes and suction powers were used for this purpose

Fig. 7 depicts the relationships between the overall efficiency of the system (E_{EPDS}) and air concentration (Q_{air}) for fine (2 mm), medium (5 mm), coarse (10 mm), large (15mm), and mixed particles using different pump pressures. The mixes particles are non-uniform

mixtures of equal volume proportions of 2 mm and 5 mm grains (i.e. 1:1 bulk volume). As shown in **Fig. 7a,** increasing Q_{air} was associated with a continuous improvement in efficiency for the 2 mm sediments. The overall efficiency of the system in removal of medium and large (15 mm) sediments exhibited some fluctuation over the same range of air injections (**Fig. 7b**). For these sediments there seems to be an optimum air concentration range for the highest observed (E_{EPDS}). Indeed, the higher Q_{air} intensified the suspension of fine sediments into the slug flow body allowing them to be carried a longer distance in the slug flow. The dredging system exhibits its best performance when an intermediate concentration of air between 40 to 80 nl/min were used.

The total superficial velocity (J) and efficiency (E_{EPDS}) were calculated for 11 selected cases (different sediment sizes, and pump pressures) using a range of air concentrations**.** It was found that raising the air concentration has increased J values for all cases (**Fig. 8a**), but not necessarily E_{EPDS} (**Fig. 8b**). More specifically, increasing Q_{air} for large and medium size sediments (cases 1 to 7) was not consistently associated with a corresponding increase in E_{EPDS} – contrary to finer sediments (cases 8 to 11). This is attributed to their distinct transport pattern in EPDS. As compared to large sediments, the success in boosting the efficiency of medium-size sediments is more dependent on the air concentration. The relation between the injected air into the transport pipeline and the maximum Q_s is shown in **Fig. 9**. The maximum Q_s increased with increasing Q_{air} up to approximately 60 nl/min then decreased with further increase in air injection. The maximum observed Q_s for 2 mm sediments is higher than that of 5 mm particles. In both cases, there seem to be an optimum air injection between 40 and 80 nl/min.

Synopsis

The proposed system provides a number of solutions and advantages over traditional suction dredging systems. The use of a high-pressure water jet in lieu of a blade-rotary pump for

278 generating a negative pressure (suction) allows unsupported removal of sediments. The ejector
279 pump is less likely to jam, rust or breakdown because of the absence of wings (impellers).
280 Injection of air has proven to be instrumental for ensuring continuous dredging and minimizing
281 system plugging commonly observed in other suction dredging systems.

282 Air injection forms a slug flow regime, which consequently keep the sediments in
283 suspension – creating the most economical sediment transportation. The air bubbles have dual
284 roles. First, they cluster in the upper part of the pipeline, which reduces the effective cross
285 section available to flow and, hence, increases flow velocity at the same pumping capacity.
286 Second, they are likely to be absorbed or entrapped between the sediment particles. This allows
287 a range of positive consequences: reduction of the sediment density enhances resuspension in
288 the system, and reduction of the settling velocity for particles already suspended in the wavy
289 flow. Hence, sediments can be transported for a long distance by the created wave.

290 The experimental observations have shown that the removal mechanisms for coarse
291 and fine sediments in EPDS are different – particularly at low pump discharge pressures. When
292 no air introduced in TP, fine sediments tends to form dunes along the transport pipeline,
293 whereas coarse sediments are transported more individually. Coarse particles exhibit friction
294 against the flow and can be hardly suspended in the slug flow body. This explains their lower
295 removal rate compared to fine sediments. On the other hand, the clustering of fine sediments
296 (cloud-like) creates higher resistance to the flow and consequently greater pressure gradient.
297 Therefore, the risk of pipeline blockage in the absence of air injection in TP is higher for fine
298 sediments compared to that of the coarser sediments.

299 **Field Implementation**

300 The field trials of EPDS were mainly performed at the reservoirs of the Mimi River located at
301 Miyazaki Prefecture, southeast of Kyushu, Japan. The trials include suction dredging in Saigo,
302 Morotsuka and Yamasubaru reservoirs, sediment transport and gravel capping in Oouchibaru

303 reservoir, and sediment relocation in Yamasubaru reservoir. The Mimi River has a total length
304 of 94.8 km and a watershed area of 884.1 km^2. Dams in the Mimi River basin have undergone
305 upgrading and retrofitting post Typhoon Nabi in 2005 to increase flow and sediment release
306 (Kantoush and Sumi, 2016). **Fig. 10** depicts the location of the hydropower dams and
307 reservoirs considered in the field trials (Yamagami et al., 2012).

308 The results of the laboratory phase provided a solid proof of concept to build two full-
309 scale EPDS setups for sediment removal and relocation. The suction-type EPDS is used to
310 remove the deposited sediments from the bottom of a reservoir and transport them to the
311 downstream area, while the hopper-type EPDS can be used to relocate collected or stored
312 sediments to a desired disposal site. The following section provides a description of the full
313 scale EPDS components and configurations.

314 **System Components**

315 The main components of the field EPDS system is comprised a high-pressure pump, ejector
316 pump, air compressor, transport pipeline and distributing shipboard (**Fig. 11a**). The high-
317 pressure pump and air compressor were set to inject 1 to 3 water units and 0 to 1 air units,
318 respectively, into the system (1 unit is 18 m^3/min). The ejector house is designed to serve dual
319 functions. First, suck the sediments from the bottom of reservoir and transport them to the
320 downstream area (suction-EPDS). Second, transport the collected sediments to a disposal area
321 without suction (hopper-EPDS). The driving force of the system from the high-pressure pump
322 to the ejector pump is shown in **Fig. 11b**. The distributing shipboard is set at the end of transport
323 pipeline to release the sediments (**Fig. 11c**). The distributor is used to keep the transport
324 pipeline on the water surface using several sets of float tube attached to the pipe segments. Silt
325 fences were installed to a depth of 5 m below the water surface to minimize turbidity and water
326 pollution during sediment dredging and deposition (**Fig. 11c**).

327 **System Configurations and Parameters**

328 The suction-EPDS is equipped with a 220-kW pressure pump that discharges a high velocity
329 water jet into the ejector house through a nozzle to create a negative pressure (suction). At a
330 flow rate of approximately 5 m^3/min, the pump creates an equivalent suction pressure of 1.95
331 MPa. As shown in **Fig. S3**, the hopper-type EPDS assembly mounted on the shipboard hosts a
332 conveyor belt that feeds the dredged (or stored) sediments for disposal through a hopper
333 attached to the ejector. The sucked or stored (after dredging) sediments are subsequently
334 discharged to a designated sediment tank. The ejector is equipped with an air controller inlet
335 and a straight inner pipeline to eliminate cavitation as well as abrasion of the system. The air
336 inlet valve (detail "**A**" in **Fig. S3**) has three settings: closed, half-open, and fully open. The
337 transport line consists of 6-m long 400-mm PVC pipe segments connected to each other by 1-
338 m long rubber links for flexibility (**Fig. 11a**). The system parameters and measuring devices
339 are shown in **Fig. S3** (also included in the notations).

340 **Sediment Removal**

341 In the case of Morotsuka reservoir, dredging was performed in 4 to 9 m deep water using 5, 10,
342 15 and 20 m long suction pipes. Yamasubaru reservoir was dredged by lowering the EPDS
343 under the water surface.

344 Various configurations of these EPDS, such as water pressure of the jet pump,
345 diameter of the suction pipe, suction height, inner pipe diameter, were used. The system
346 performance was evaluated by investigating the relationship between the flow rates ($Q1$ and
347 $Q2$), water head, and pressures $P1$ and $P2$. Two sets of high-pressure pumps capable of
348 producing a combined $Q1$ of 10-11 m^3/min were used. The system was tested at pump
349 pressures $(P1)$ of 0.8, 1.0, 1.3 and 1.5 MPa for ejector's inner pipes of 200 and 250 mm. The
350 associated suction flow $(Q2)$ ranged from 7.9 to 12 m^3/min and the measured pressures in the
351 transport pipe ($P2$ and $P3$) varied from 0.08 to 0.18 MPa.

352 Evaluation of the dredging efficiency in Morotsuka reservoir was furnished by

353 considering different suction pipe sizes, ejector depths, applied flow rates ($Q1$) with and
354 without air injection. As shown in **Fig. 12**, the flow rate ($Q2$) increases with the pump
355 pressure, with generally a better response for 250-mm inner diameter than the 200-mm one.
356 Plugging occurred in the transport pipeline when no air was injected into the system. The fully-
357 open air valve minimized plugging in the pipeline, but the flow rate was reduced. For half-open
358 valve and 200-mm inner diameter, there is no notable increase in flow rate with increasing $P1$
359 beyond 1.1 MPa. At the low $P1$ values, the flow associated with the 200-mm diameter was
360 higher than that of the 250-mm. Therefore, the former was perceived more efficient.

361 The relation between $Q2$ and water head of the system is shown in **Fig. 13**. The
362 measured flow rate was almost the same for both pipe diameters at a water head of
363 approximately 10 m. The 200-mm size outperformed the 250-mm diameter for larger water
364 heads, up to 21 m. The high head (pressure) associated with the use of the small inner pipe is
365 obviously advantageous for transportation ability of the system. The productivity was 120
366 m^3/h for 100-m long transport line. However, for water heads less than 10 m and short
367 transportation, the use of a large inner pipe is preferred for easier removal of the large
368 sediments.

369 The vertical position of the ejector pump with respect to the reservoir's bed can be
370 adjusted using a lifting arm. The effect of the ejector's depth below water surface on $Q2$ was
371 investigated at a pump pressure of 1.86 MPa using a 15-m long suction pipe (**Fig. 14**). Two
372 suction depths were examined: 7 m and 11 m. The relationship between the water depth and
373 sediment transportation rate for all 58 cases was closely studied (**Fig. S4**). Similar to
374 conventional hydraulic suction, locating the ejector pump deep under the water surface
375 improved the suction efficiency of the system.

376 The excavated sediments from Oouchibaru reservoir were screened using 80 mm and
377 120 mm sieves to remove cobbles (**Fig. S5**). A screw crusher (**Fig. S3**) was used to break down

the large driftwood into smaller pieces of approximately 150 mm prior to removal by EPDS. The crusher's shaft disintegrated the gravels entering in-between the conical shaped shaft and the lining plates in the shell. This allowed a convenient removal of sediment sizes that could not be tackled using conventional submersible water pumps. Given the wide size range of sediments and driftwood, mechanical sieving was necessary to split the dredged sediments into two size fractions: smaller and larger than 100 mm. Oversized material was transported to the Oouchibaru reservoir for gravel capping. The maximum size of gravel that removed by EPDS was around 150 mm. This highlights the need for a modifying the EPDS to make it capable of removing coarser sediment larger than this size. The system, however, did not experience plugging nor over-dredging.

Sediment Transport and Relocation

The relation between the pressure at the starting point of the transportation pipeline ($P1$) versus the sediment transportation rate (S) is shown in **Fig. 15a** for the hopper-type EPDS. The observed transportation rates are linearly proportional to the pressure for three transportation lengths (L_{tp}) of 200, 600, and 1,000 m. The transportation rate decreased exponentially with the length (**Fig. 15b).** This highlights the significant adverse effect of L_{tp} on sediment transport efficiency. Combining the two factors**,** the sediment removal rate is linearly proportional to $P2/L_{tp}$ (**Fig. 15C).**

The air injected into the transportation pipeline was set at 36 and 54 nm^3/min for 600 and 1,000 m transport pipeline, respectively. For the initial water discharge of about 10 m^3/min, the ratio of the injected air into the system to the water discharge was approximately 3 to 6. At those air concentrations, the measured removal rates were approximately 30 and 50 m^3/h for transport pipe lengths of 600 m and 1,000 m, respectively. Based on the collected measurements, the maximum water head of the ejector pump is assumed proportional to the

ratio of the nozzle to inner pipe sectional area ($\frac{D_n^2}{D_i^2}$) and the pump pressure. The estimated pressure at the starting point of the transportation pipeline (T) can therefore be expressed as follows:

$$T = \left(\frac{D_n^2}{D_i^2}\right) P_1 + \alpha \quad (11)$$

Where D_n is the nozzle diameter, D_i is the inner pipe diameter, and α is a constant. The estimated pressure (T) is almost equal to the pressure $P2$ at α value of 0.067 (**Fig. 15c)**. This assumption holds for nozzle and inner pipe diameters ranging from 58 to 70 mm and from 200 to 250 mm, respectively. Within these ranges, the high-pressure pump delivers its energy proportional to $\frac{D_n^2}{D_i^2}$ ratio. The sediment transportation rate (S) can be related to the estimated $\frac{T}{L_{tp}}$ ratio as follows (**Fig. 15c**):

$$S = 93.8\frac{T}{L_{tp}} + 7.71 \quad (12)$$

This relation between the estimated S and $\frac{T}{L_{tp}}$ is supported by the best fit of the field measurements as shown in **Fig. 15c**. Substituting **Eq. (11)** into **Eq. (12)** yields:

$$S = \frac{93.8}{L_{tp}}\left[\left(\frac{D_n^2}{D_i^2}\right) P1 + \alpha\right] + 7.71 \quad (13)$$

By simple manipulation of **Eq. (13)**, the required pump pressure ($P1$) of the system can be accordingly estimated:

$$P1 = \left[\frac{L_{tp}(S-7.71)}{93.8} - \alpha\right]\frac{D_i^2}{D_n^2} \quad (14)$$

This equation can be used to estimate the pumping power needed to deliver a desired sediment removal rate (S) for a given set of geometrical configurations of the transport line $\left(\frac{D_i^2}{D_n^2}\right.$ and $\left.L_{tp}\right)$. For example, if the targeted S is 50 m^3/h and a 1.0 Km transportation pipe having a $\frac{D_i^2}{D_n^2}$ ratio of 8.1 ($based\ on\ D_i = 200mm\ and\ D_n = 70mm$) is used, a 3.1 MPa

pumping pressure is needed.

The dredged sediments were transported to closely investigate the performance and efficiency of the hopper-type dredger in the trial tests conducted in the Saigo reservoir. These sediments were relocated to a maximum transportation length of 1,000 m using a hopper attached to the ejector pump and a conveyor belt extended to the disposal area downstream of Oouchibaru reservoir. The grain size analysis of the fine portion of the dredged sediment has shown that 88% of removed particles fell between 0.425 to 0.85 mm, with a mean size of 0.39 mm. The dredged material also included stone, gravel, branches and debris. As a result of relatively long suction pipeline, system blockage was encountered. The ejector pump was placed under the water surface to enhance suction. Thus, the distance between the ejector pump and entrance of suction pipeline (reservoir bed) can be adjusted to reduce the risk of sediment plugging. The EPDS was able to lift 3,500 m^3 of sediments from reservoir's depths ranging from 3 to 15 m. The dredged sediments were subsequently relocated using a floating transportation pipeline to the disposal site, located 400 m upstream of the suction point.

Embracing Sustainable Sediment Management

An integrated sediment management plan was implemented to ensure sustainable upgrading of the Mimi River Basin. The EPDS system was utilized for sediments removal and relocation, and subsequent capping along the retrofitted dam sites (Turusaki et al., 2017). This solution has successfully restored and upgraded the Yamasubaru, Saigou and Oouchibaru dams (**Fig. S6**).

Sluicing in the upstream of the Oouchibaru Dam was carried out in 2015. A total volume of 107,600 m^3 of gravel and sand capping was placed at the reservoir's bed before sluicing in order to combat possible high turbid water release on the downstream. Therefore, controlling and monitoring of turbidity were performed during construction. Turbid water

448 generation was analyzed and estimated considering the material of gravel capping, method of
449 execution, and the diffusion properties of the turbid water outflow. The dredged material caps
450 were placed in the reservoir by using the hopper-type EPDS.

451 It is expected that the turbidity level will decrease with the distance from the dredger
452 and the reservoir bed. **Fig. 16** displays the turbidity levels (in terms of the suspended sediment
453 concentration-SSC) at different times during dredging. The turbidity was monitored at different
454 distances from the sediment injection point on both sides of the silt fence. Surface SSC values
455 were the lowest for all turbidity measurements at different locations away from EPDS point
456 (**Fig. 16a**). The values of SSC declined quickly with the distances from EPDS for all depths. A
457 maximum turbidity of about 200 mg/l was measured at 5 m below the surface just at the EPDS
458 (**Fig. 16b**). This value dropped below 50 mg/l at 150 m from EPDS point. Furthermore, there
459 no 'plumes' were observed behind EPDS for all full-scale pilot test. These observations
460 collectively indicate an eco-friendly performance of the system and, ultimately, a minimal
461 impact on the reservoir environment.

462 **System Optimization and Merits**

463 The EPDS system provides a range of desirable characteristics and merits in sediment
464 management programs. The eco-friendly performance of the system makes EPDS over-shines
465 all comparable dredging systems from the environmental standpoint. It works effectively as
466 one unit up to a distance of 1,000 m from the suction point with no need for a booster. The
467 production of the suction-type and hopper-type EPDS system depends on the pump flow rate,
468 ejector's depth and inner pipe diameter, and injected air concentration, which can be adjusted
469 to maximize productivity. Therefore, the three types of field implementations (dredging,
470 sediment transport with gravel capping and sediment relocation) in Japanese reservoirs were
471 quite helpful in testing the proposed "optimal" design of the system.

472 Field trials indicated that the maximum production for sandy and gravelly sediments

473 can be achieved with air injections of 36 and 54 nm^3/min for transport lengths of 600 and 1,000
474 m, respectively. The system allows uninterrupted (no plugging) sediment removal in water
475 depths up to 20 m with a dredging capacity up to 70 m^3/h and 35 m^3/h in sandy and gravelly
476 soils, respectively. The optimum dredging production rate occurs at a pumping capacity of
477 about 10 m^3/min, using a 200 mm ejector's inner pipe for suction lengths less than 8 m, and air
478 concentrations of 40-60 nm^3/min. The maximum sediment removal using EPDS-Hopper type
479 can be estimated from **Eq. (13)**. In order to dredge various sediment types including hard clay
480 and sandy sediments with greater depth (50-100 m) it is necessary to break down these
481 materials using the auxiliary horizontal multi-axis cutter. The cutter can be replaced with a
482 crusher to be adapted to various sediment conditions, which can include wood, clay, sand and
483 rock.

484 A comparison between the proposed EPDS and the commercially available hydraulic
485 suction dredging systems is shown in **Table 2.** Generally, conventional suction dredgers yield
486 33 m^3/h in sandy soils with no reported success in gravelly soils. For instance, the suction
487 system by hydro-jet pump has the lowest cost and provides the highest productivity. However,
488 it is suitable only for fine sediment and for limited transportation length. Likewise, the siphon
489 dredging has a limited dredging depth with a high potential of clogging in the transportation
490 pipeline. The cost and production are highly variable as they are site specific, i.e. controlled by
491 the transport distance to relocating sites, reservoir bathymetry, and types of bed sediments. In
492 view of the limitations and pros and cons in each method, the cost and production comparison
493 should be merely used as an indicator.

494 The injection of air into the EPDS system was instrumental for efficient dredging of
495 fine and medium size deposits – the most commonly encountered sediments – using low
496 suction powers. This reduces the dredging cost and time and allows sediment transport for
497 longer distances. The cost of dredging falls within those of the suction systems as reported in

Table 2. Compared to other systems, however, the productivity and cost effectiveness of the EPDS system are very attractive, particularly owing to its low maintenance, limited environmental impact and versatility.

Closing Remarks

Continuous sediment deposition is a major recurring issue that hampers sustainable management of reservoirs. Due to the decreasing availability of suitable new dam sites, raising existing dams is always considered as a practical solution to cope with the increasing water storage demand. However, this approach poses socio-environmental threats to the habitat and public safety. To this end, it is imperative to adopt a holistic vision honoring sustainability and eco-friendly sediment management. The current study suggests a viable suction dredging technique for an integrated sediment management of dam reservoirs. Combined with sediment bypassing, the sediment removal using the proposed EPDS can reduce the magnitude and frequency of the required dredging. The three components (driving force, suction, and transportation) of the proposed EPDS work as an integrated unit for sediment dredging and transport in reservoirs of different sizes. The system has proven efficient dredging of coarse and fine sediments in both laboratory experimentation and field trials. Its simplicity and mobility allow versatile operations in remote or mountainous reservoirs. The EPDS system can be used to dredge and relocate the sediments within the reservoir near dam sites and intake structures – with limited turbidity levels at the dredging and disposal points as well as during gravel capping operations.

Acknowledgements

The first two authors have equally contributed to this manuscript. The experimental work of this research was conducted at Taiwan International University with collaboration of Ando Hazama Corporation and POJET co. The authors are indebted to the invaluable input and field

522 trials performed by our industry partners. It is also inevitable to acknowledge Mr. Sandun
523 Dassanayake, PhD candidate at Monash University Malaysia, for conducting some editorial
524 tasks and providing additional references that supported our views and findings.

525 **Data Availability**

526 All data, models, and code generated or used during the study appear in the submitted article
527 and the supplemental material.

528

Notation

A_p = Cross-sectional area of transport pipeline (m^2);

C_{ss} = Concentrations of sediment removal in suction pipeline (%);

C_{st} = Concentrations of sediment removal in transport pipeline distance (%);

d_s = Sediment grain size (mm);

D_{sp} = Internal diameter of suction pipe (mm);

D_{tp} = Diameter of the transport pipeline (mm);

D_n = Diameter of the nozzle (mm);

D_i = Diameter of inner pipe (mm);

E_{EPDS} = Overall efficiency of system performance (%);

H_{suc} = Height of the suction vertical pipeline (m);

H_{sp} = Height of the suction pipeline (m);

J = Total superficial velocity in the transport pipeline (m/s);

J_A = Superficial air velocity in the transport pipeline (m/s);

J_W = Superficial water velocity in the transport pipeline (m/s);

L_{sp} = Length of the suction pipeline (m);

L_{tp} = Length of transport pipeline (m);

$P1$ = Initial pressure of water measured by pressure gauges located at the pump (kPa);

$P2$ = Pressure measured at the beginning of the transport pipeline (kPa);

$P3$ = Pressure measured at the end of the transport pipeline (kPa);

P_{pump} = Pump discharge pressure (kPa);

Q_{suc} = The suction power (volume of water and sediment lifted during a specific time period (l/min) - or water-sediment sucked from the reservoir);

Q_{air} = Injected air concentration to the transport pipeline *(nl/min)*;

553 Q_s = Sediment discharge (transportation) rate for suction-type (*l/min*);

554 Q_{pump} = Discharge of pump (*l/min*);

555 Q_{ws} = Discharge of water-sediment through the transport pipeline (*l/min*);

556 $Q1$ = Initial discharge measured by a flowmeter (*l/min*);

557 $Q2$ = Flow rate in the suction pipeline measured by flowmeter (*l/min*);

558 S = Sediment transportation rate for hopper-type EPDS (volume of sediment placed on
559 the bottom of the reservoir per hour)

560 t_{ws} = Time needed for suction and removal of water and sediment at the end of transport
561 pipe (S);

562 V_s = Volume of sediments initially placed in the storage tank (liter);

563 V_{ws} = Volume of released water and sediment (l);

564 Δx = Distance between two piezometers/pressure probes;

565 ρ_s = Density of sediment (kg/m^3); and

566 ρ_w = Density of water (kg/m^3)

567 **Supplemental Materials**

568 Figs. S1–S6 are available online in the ASCE Library (ascelibrary.org).

569

570 **Fig. S1.** Superficial velocities of air (J_A) and water (J_w) and flow pattern map in two-phase flow
571 (chart from Mandhane et al.,1974; Taitel and Dukler, 1976).
572
573 **Fig. S2**. Sediment removal (C_{st}) vs pressure gradient ($\partial p/\partial x$) for air concentrations of: (a) 0
574 nl/min; (b) 25 nl/min; (c) 60 nl/min (P_{pump}=*588 kPa,* L_{tp}= *7 m*).
575
576 **Fig. S3.** Sediment dredging system using suction-type and hopper-type EPDS.
577
578 **Fig. S4**. Water depth and sediment transportation rate through suction (Q_s).
579
580 **Fig. S5.** Grain size distribution of sediments.
581
582 **Fig. S6**: Utilization of EPS for managing the sediment within the reservoir by re-locating,
583 dredging to the downstream, dredging to sediment recycling, and through the spillway. The

584 EPS can be associated with other structures as sediment bypass tunnels and sediment capping
585 for environmental purposes during sluicing.

586 **References**

587 Auel, C., S. A. Kantoush, and T. Sumi 2016. "Positive effects of reservoir sedimentation
588 management on reservoir life-examples from Japan." *84th Annual Meeting of ICOLD*.

589 Bray, R.N., A.D. Bate., and J.M. Land, 1996. "Dredging: A Handbook for Engineers." *2nd*
590 *Ed. Butterworth-Heinemann*.

591 Basson, G.R., A. Rooseboom, 1999. "Dealing with reservoir sedimentation: dredging. South
592 Africa." *Water Research Commission, WRC report*, no. TT 99/110, ISBN:1868454932
593 9781868454938

594 Bruk, S. 1985. "Methods of computing sedimentation in lakes and reservoirs: a contribution
595 to the International Hydrological Programme, IHP-II Project A. 2.6. 1. panel." *Methods of*
596 *computing sedimentation in lakes and reservoirs: a contribution to the International*
597 *Hydrological Programme, IHP-II Project A. 2.6. 1. panel*, Unesco.

598 Chaudhuri, B., A. Ghosh, B. Yadav, R. P. Dubey, P. Samadder, A. Ghosh, A. Das, S.
599 Majumder, S. Bhandari, N. Singh & S. Das. 2020. "Evaluation of dredging efficiency indices
600 of TSHDs deployed in a navigational channel leading to Haldia Dock Complex." *ISH Journal*
601 *of Hydraulic Engineering*, DOI: 10.1080/09715010.2020.1786738

602 Dabirian, R., R. Mohan, O. Shoham, G. Kouba. 2016a. "Critical sand deposition velocity for
603 gas-liquid stratified flow in horizontal pipes." *J. Nat. Gas Sci. Eng.* 33, 527e537

604 Dabirian, R., R. Mohan, O. Shoham, G. Kouba. 2016b. "Solid-particles Flow Regimes in
605 Air/Water Stratified Flow in a Horizontal Pipeline." *Oil and Gas Facilities*, pp. 5e06

606 Fu-sheng, N., Z. Li-juan, G. Lei, J. Shuang, Q. Li-na, X. Li-qun, H. Kun-jin, L. Rui-xiang,
607 and Z. Quan-sheng. 2010. "Simulation of dredging processes of a cutter suction dredger."
608 *2010 International Conference on Audio, Language and Image Processing*, 628–632.

609 Gillies, R. G., M. J. McKibben, and C. A. Shook. 1997. "Pipeline flow of gas, liquid and sand
610 mixtures at low velocities." *Journal of Canadian Petroleum Technology*, Petroleum Society
611 of Canada, 3609.

612 Goharzadeh, A., P. Rodgers, and C. Touati. 2010. "Influence of Gas-Liquid Two-Phase
613 Intermittent Flow on Hydraulic Sand Dune Migration in Horizontal Pipelines." *Journal of*
614 *Fluids Engineering*, American Society of Mechanical Engineers, 1327, 71301.

615 Herbich, J. B. (editor) 2000. "*Handbook of dredging engineering*." McGraw-Hill Co., New
616 York, 2nd edition.

617 Kantoush, S. A., A. J. Schleiss, T. Sumi, and M. Murasaki. 2011. "LSPIV implementation for
618 environmental flow in various laboratory and field cases." *Journal of Hydro-environment*
619 *Research*, Elsevier, 54, 263–276.

Kantoush, S. A., and T. Sumi. 2016. “The Aging of Japan’s Dams: Innovative Technologies for Improving Dams Water and Sediment Management.” *Proc. 13th International Symposium on River Sedimentation ISRS, Stuttgart, Germany*.

Kantoush, S. A., and T. Sumi. 2019. “Paradigm shift for sediment management.” International Water Power & Dam Construction*, IHA, UK*.

Kim, T. W., T. B. Aydin, E. Pereyra, and C. Sarica. 2018. “Detailed flow field measurements and analysis in highly viscous slug flow in horizontal pipes.” *International Journal of Multiphase Flow*, Elsevier, 106, 75–94.Leporini, M., B. Marchetti, F. Corvaro, G. di Giovine, F. Polonara, and A. Terenzi. 2018. “Sand transport in multiphase flow mixtures in a horizontal pipeline: An experimental investigation.” *Petroleum*, Elsevier, 52, 161–170.

Lewis, J. M., and R. E. Randall. 2015. “Prediction of Minor Loss Coefficient at Suction Inlet of Cutter Suction Dredge.” *Journal of Dredging, Western Dredging Association WEDA*, 151, 14–42.

Mandhane, J. M., G. A. Gregory, and K. Aziz. 1974. “A flow pattern map for gas—liquid flow in horizontal pipes.” *International Journal of Multiphase Flow*, Elsevier, 14, 537–553.

Meshkati Shahmirzadi, M. E., T. Sumi, S. Kantoush, and T. Temmyo. 2012. “Influence of Air Injection on Suction Power and Pressure Gradient in Dredger System.” *Journal of Japan Society of Civil Engineers, Ser. B1 Hydraulic Engineering*, Japan Society of Civil Engineers, 684, I_37--I_42.

Morris, G. L. 2020. "Classification of management alternatives to combat reservoir sedimentation." *Water 12(*3): 861.

Nakamura, Y., T. Okabe, T. Temmyo, T. Yamashita, M. Kaku, Y. Yamagami, O. Kuroki, T. Sumi, A. K. Sameh, and M Mohammad. 2012. “A Method of Sediment Transportation by Special Ejector Pump System in the Dam Reservoir.” *International Symposium on Dams for Changing World, ICOLD Kyoto*.

Taitel, Y., and A. E. Dukler. 1976. “A model for predicting flow regime transitions in horizontal and near horizontal gas-liquid flow.” *AIChE journal*, Wiley Online Library, 221, 47–55.

Temmyo, T., Y. Nakamura, Y. Yamagami, M. Kaku, T. Sumi, M. E. Meshkati, 2013. “Sediment relocation trial by Ejector Pump Dredger System (EPDS) in a dam reservoir.” In Proc., *12th International Symposium on River Sedimentation*, *ISRS 2013*. London: Taylor & Francis.

Tsurusaki, D., M. Kiyota, K. Asazaki, Y. Nakamura, T. Temmyo, M. Mizunuma, A. Mousa, S. A. Kantoush, T. Sumi, 2017. “Gravel Capping for turbidity control during sediment Sluicing by the use of Ejector Pump System.” *In Proc.37th IAHR World Congress*, Kuala Lumpur, Malaysia.

Turner, T. M. 1996. *Fundamentals of hydraulic dredging*. ASCE Press New York.

Yamagami, Y. 2012. “Approaches for integrated sediment flow management at dams in the mimikawa river basin.” *Inter-national symposium on dams for a challenging world, ICOLD Kyoto*.

Yaqub, M.W., R. Marappagounder, R. Rusli, R. Prasad, D.M. R. Pendyala, 2020. “Review on gas–liquid–liquid three–phase flow patterns, pressure drop, and liquid holdup in pipelines.” *Chemical Engineering Research and Design*, 159: 505-528.

Figure Captions

Fig. 1. Concept of the ejector house (EPDS).

Fig. 2. Schematic of the laboratory EPDS Prototype.

Fig. 3. Flow profile and PIV average distribution in a straight segment of transport pipe (d_s= 2 *mm*, P_{pump} = 0.196*MPa*) for: (a) Q_{air} = 0 *nl*/*min*, (b) Q_{air} = 25 nl/min, and (c) Q_{air} = 40nl/min. (top grading on ruler in cm).

Fig. 4. Sediment removal in the suction section (C_{ss}) for 2mm and 5mm particles: (a) and (b) Q_{suc}; (c) and (d) Q_s. (P_{pump} = 588 kPa, Q_{air} = 0 nl/min).

Fig. 5. Maximum sediment discharge (Q_s) for different suction pipe lengths (P_{pump} = 588 kPa, Q_{air} = 0 nl/min).

Fig. 6. Maximum sediment discharge (Q_s) for different transport pipe lengths (P_{pump} = 588 kPa, d_s = 5 mm).

Fig. 7. Effect of air concentration (Q_{air}) on the overall efficiency of the system (E_{EPDS}) using different suction powers (P_{pump}): (a) ds = 2 mm; (b) ds = 10 mm and large (15mm).

Fig. 8. Effect of air injection (Q_{air}) on: (a) total superficial velocity of the flow (J); and (b) overall system efficiency ($E_{EPDS} = Q_s/Q_{pump}$).
P_{pump} is 588 kPa; Mixed is defined as non-uniform mixtures of equal volume proportions of 2 mm and 5 mm grains (i.e. 1:1 bulk volume); Large is 15 mm.

Fig. 9. Maximum sediment discharge (Q_s) for a transport pipe length of 10 m (P_{pump} = 588 kPa) Mixed is defined as non-uniform mixtures of equal volume proportions of 2 mm and 5 mm grains (i.e. 1:1 bulk volume).

Fig. 10. Location map of dams along Mimi River Basin.

Fig. 11. Field EPDS dredging system: (a) dredging ship; (b) suction system; (c) distributor.

Fig. 12. Flow rate in suction pipe versus average pump pressure for the ejector inner pipe diameters of: (a) 200 mm; (b) 250 mm.

Fig. 13. Relation between suction flow rate (*Q2*) and water head for different ejector inner diameters.

Fig. 14. Suction flow rate (*Q2*) vs. depth of ejector below water surface using a pump pressure of 1.86 MPa and a 15-m suction pipe.

Fig. 15. Sediment transportation rate (S) using EPDS-hopper type for three transport pipe lengths (600, 800, 1000m): (a) vs P2; (b) vs L; (c) vs. P2/L.

P2 and T: measured and estimated pressure at the starting point of the transport pipe; L: transport pipe length. (Best fit line: $S = 96.8\frac{P2}{L} + 5.7$; Eq. (12): $S = 93.8\frac{T}{L_{tp}} + 7.71$*).*

Fig. 16. Results of turbidity measurements at the vicinity of the EPDS injection points at different water depths: (a) surface, (b) 5 m below the surface.

Table Captions

Table 1 Geometrical and hydraulic parameters for laboratory investigation.

Table 2 EPDS vs commercially available suction dredging systems.

Supplemental Figure Captions

Fig. S1. Superficial velocities of air (J_A) and water (J_w) and flow pattern map in two-phase flow (chart from Mandhane et al.,1974; Taitel and Dukler, 1976).

Fig. S2. Sediment removal (C_{st}) vs pressure gradient ($\partial p/\partial x$) for air concentrations of: (a) 0 nl/min; (b) 25 nl/min; (c) 60 nl/min (P_{pump}*=588 kPa,* L_{tp}*= 7 m*).

Fig. S3. Sediment dredging system using suction-type and hopper-type EPDS.

Fig. S4. Water depth and sediment transportation rate through suction (Q_s).

Fig. S5. Grain size distribution of sediments.

Fig. S6: Utilization of EPS for managing the sediment within the reservoir by re-locating, dredging to the downstream, dredging to sediment recycling, and through the spillway. The EPS can be associated with other structures as sediment bypass tunnels and sediment capping for environmental purposes during sluicing.

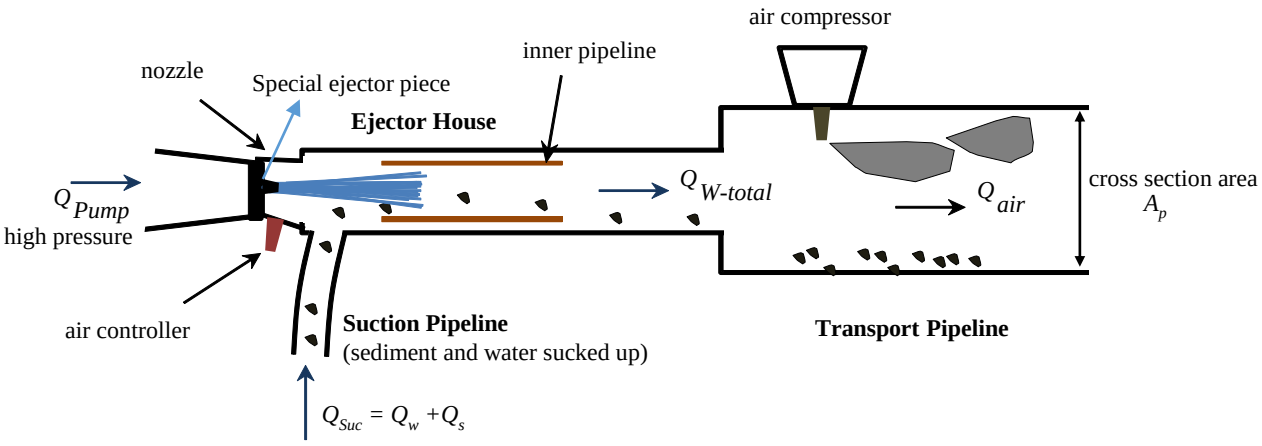

Fig. 1. Concept of the ejector house (EPDS).

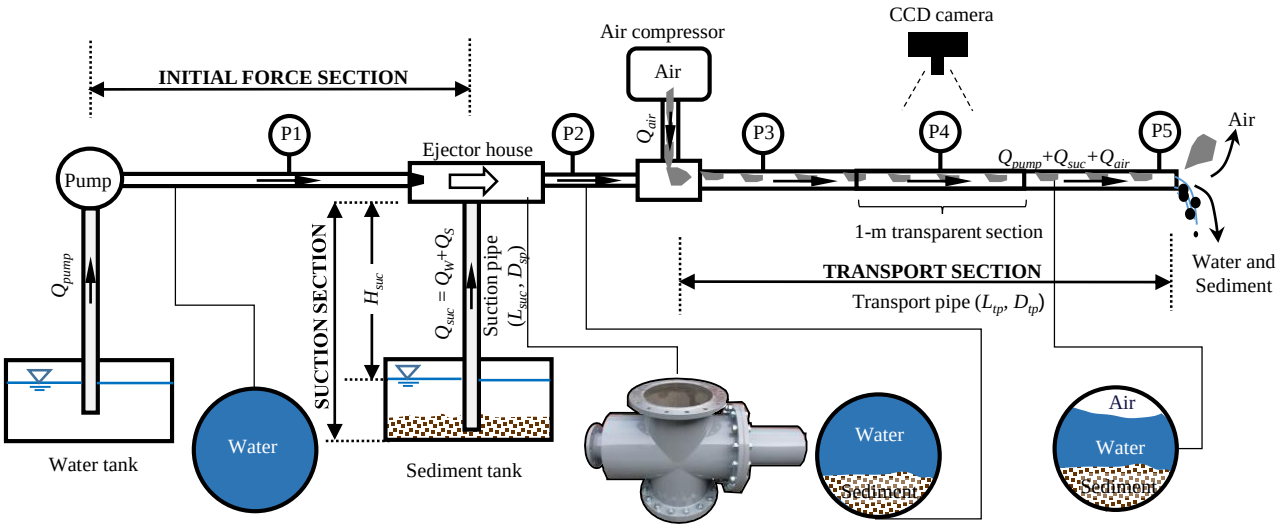

Fig. 2. Schematic of the laboratory EPDS Prototype.

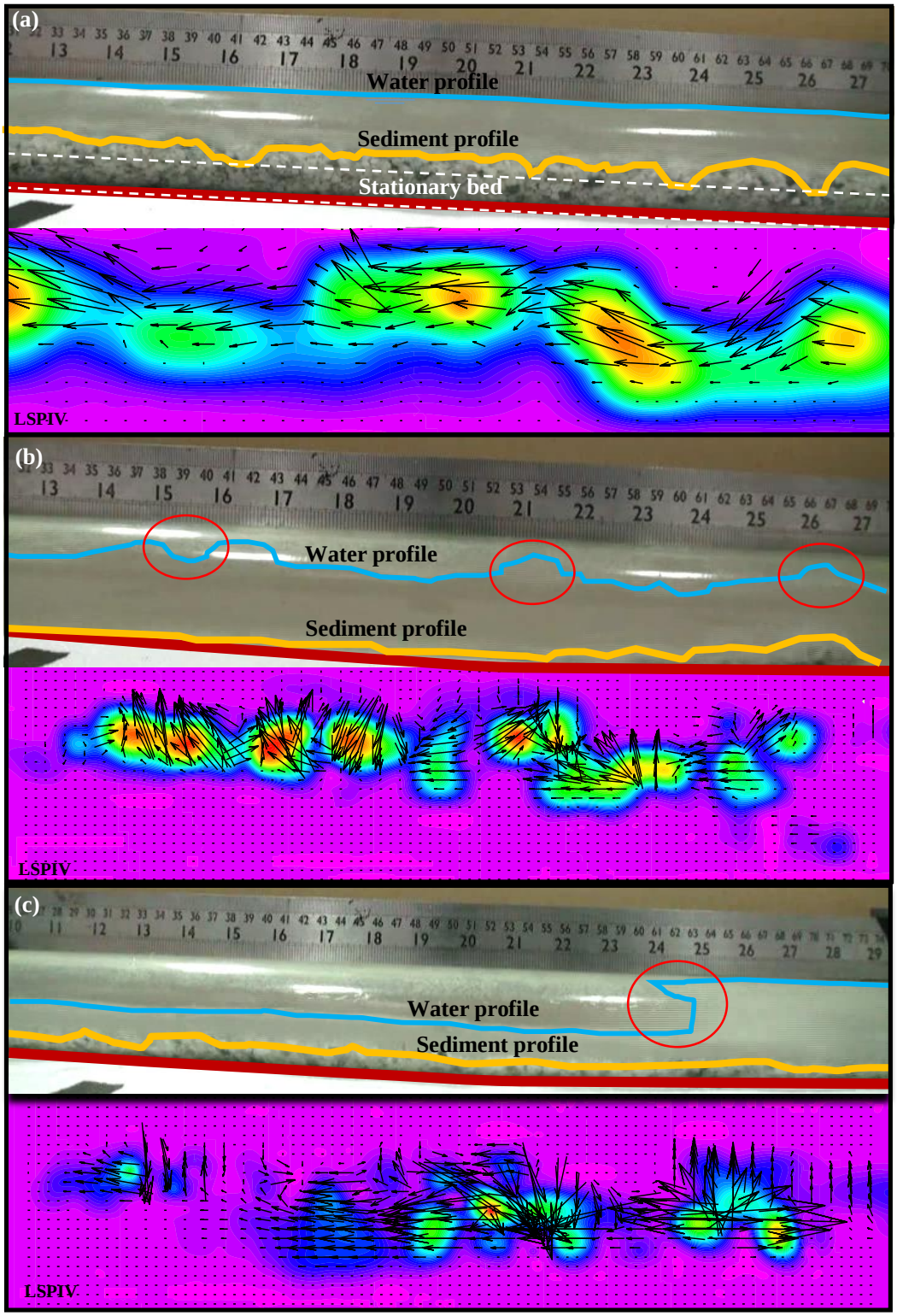

Fig. 3 Flow profile and PIV average distribution in a straight segment of transport pipe (d_s= 2 *mm*, P_{pump} = 0.196 *MPa*) for: (a) Q_{air} = 0 *nl*/*min*, (b) Q_{air} = 25 nl/min, and (c) Q_{air} = 40 nl/min. (top grading on ruler in cm).

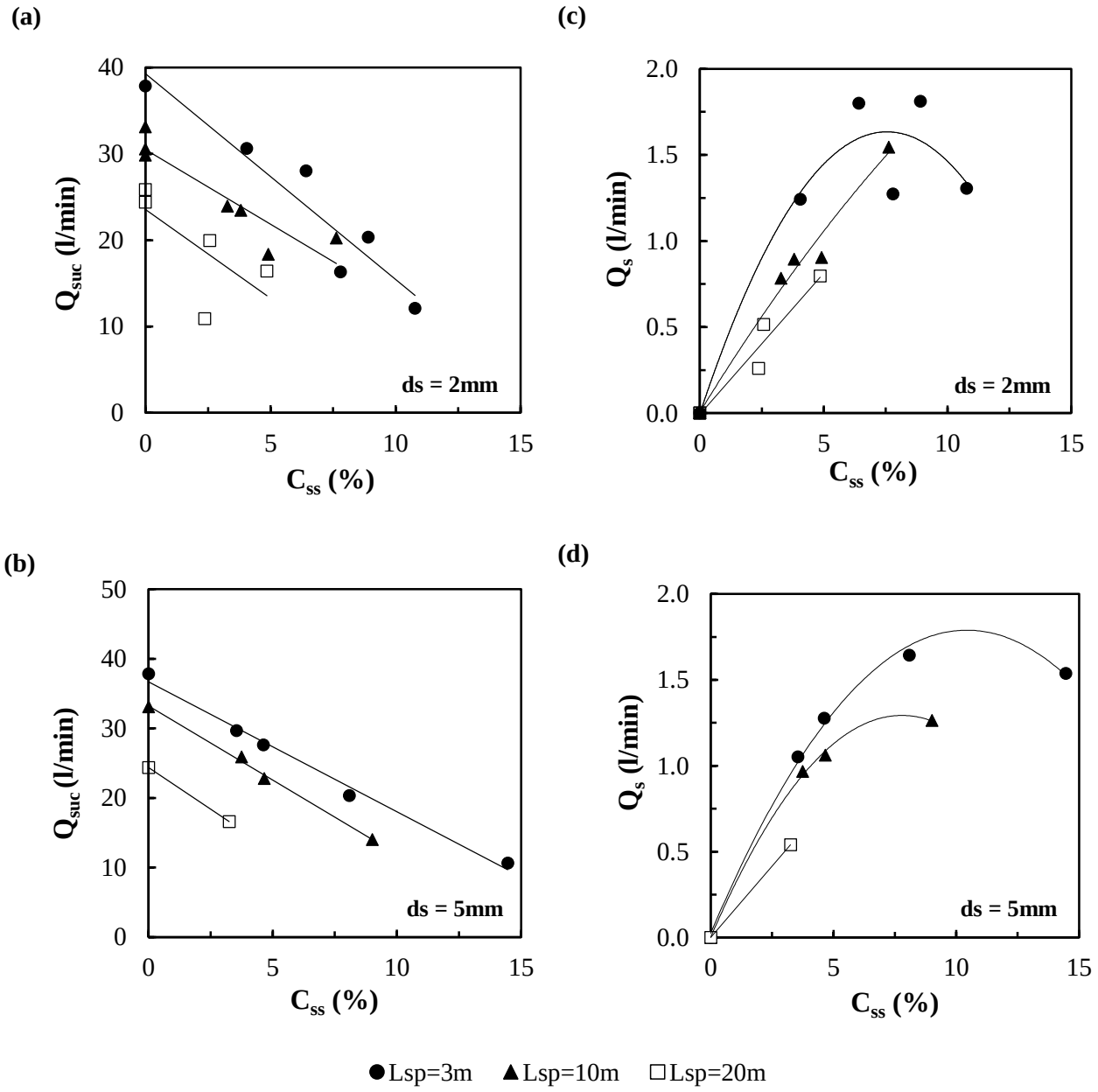

Fig. 4. Sediment removal in the suction section (C_{ss}) for 2 mm and 5 mm particles: (a) and (b) Q_{suc}; (c) and (d) Q_s. (P_{pump} = 588 kPa, Q_{air} = 0 nl/min)

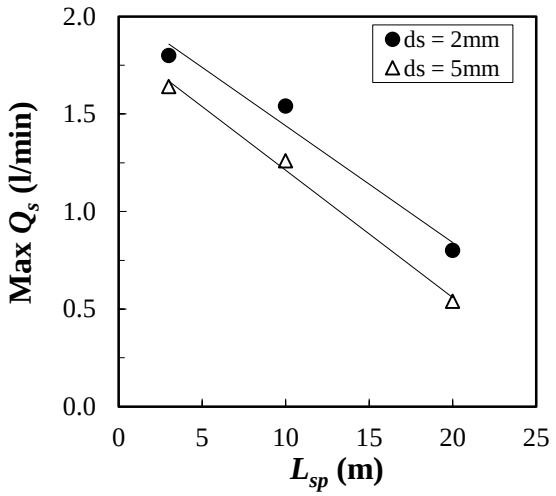

Fig. 5. Maximum sediment discharge (Q_s) for different suction pipe lengths (P_{pump} = 588 kPa, Q_{air} = 0 nl/min)

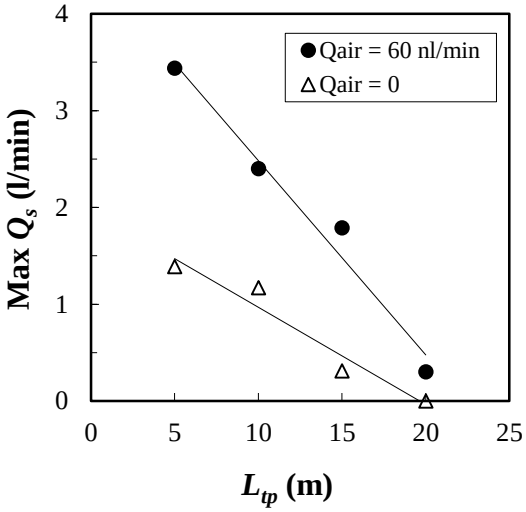

Fig. 6. Maximum sediment discharge (Q_s) for different transport pipe lengths (P_{pump} = 588 kPa, d_s = 5 mm)

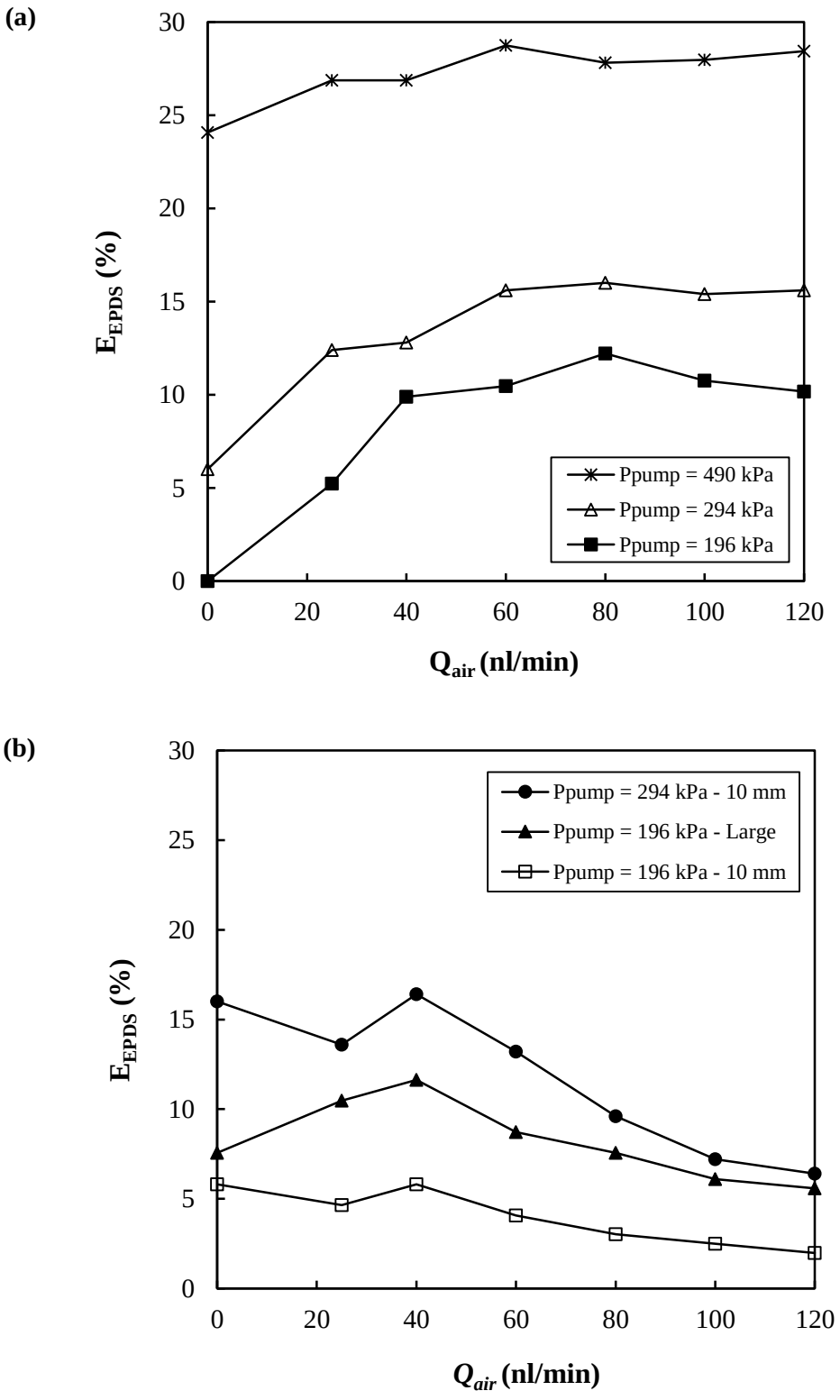

Fig. 7. Effect of air concentration (Q_{air}) on the overall efficiency of the system (E_{EPDS}) using different suction powers (P_{pump}): (a) ds = 2 mm; (b) ds = 10 mm and large (15mm).

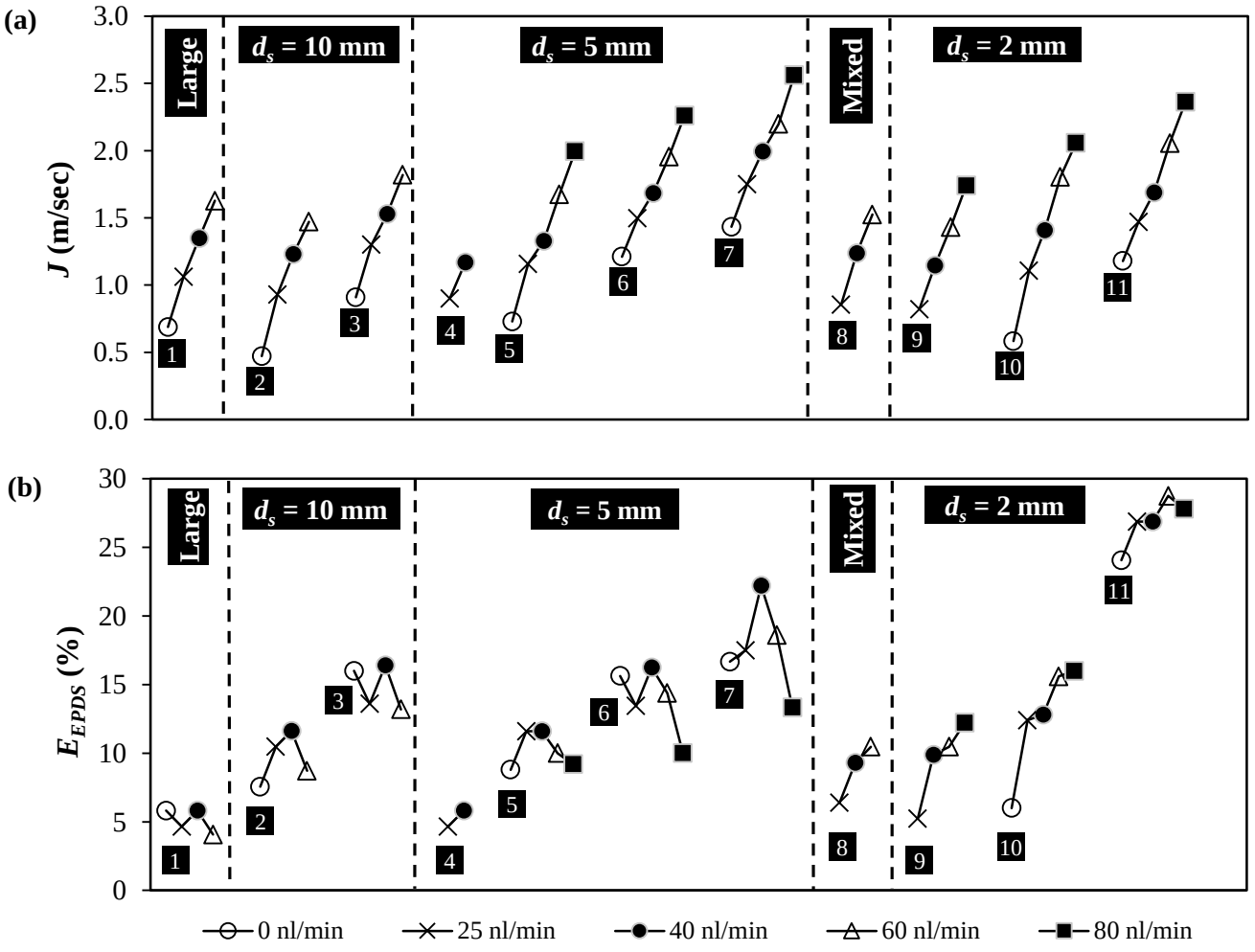

Fig. 8. Effect of air injection (Q_{air}) on: (a) total superficial velocity of the flow (J); and (b) overall system efficiency ($E_{EPDS} = Q_s/Q_{pump}$).
P_{pump} is 588 kPa; Mixed is defined as non-uniform mixtures of equal volume proportions of 2 mm and 5 mm grains (i.e. 1:1 bulk volume); Large is 15mm

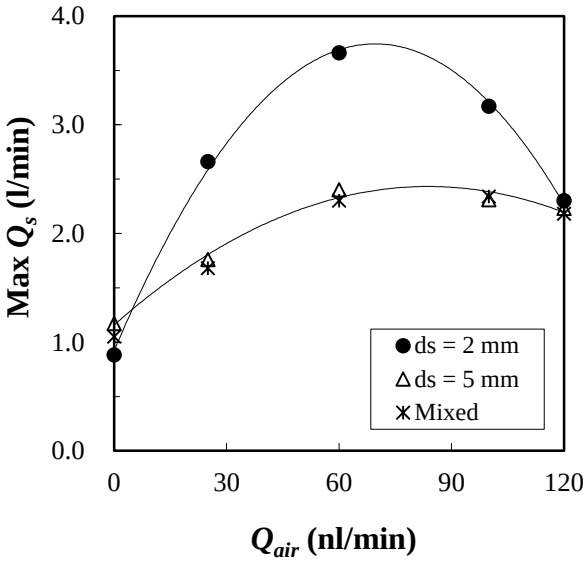

Fig. 9. Maximum sediment discharge (Q_s) for a transport pipe length of 10 m (P_{pump} = 588 kPa)
Mixed is defined as non-uniform mixtures of equal volume proportions of 2 mm and 5 mm grains (i.e. 1:1 bulk volume)

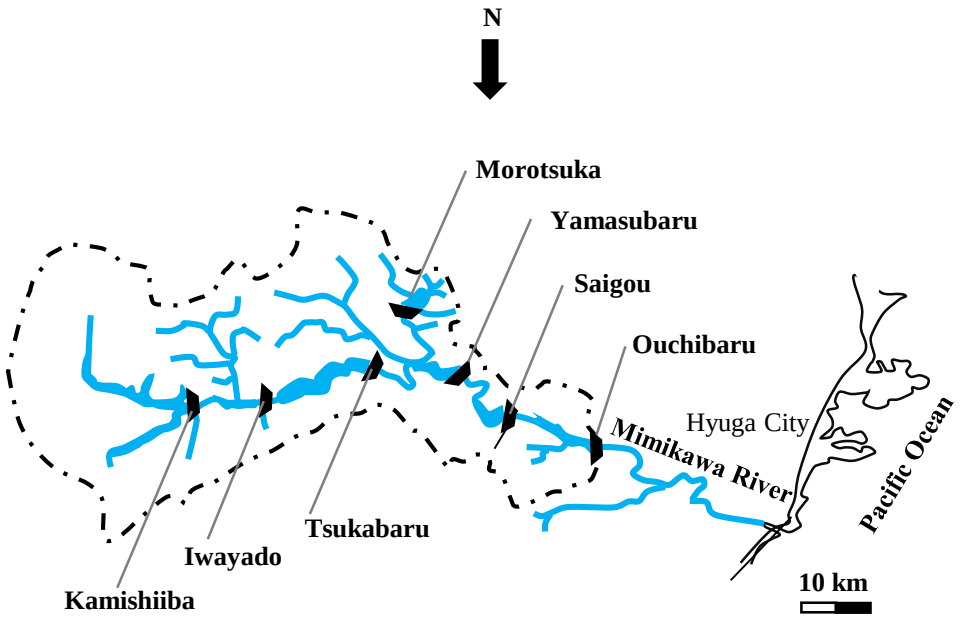

Fig. **10.** Location map of dams along Mimi River Basin.

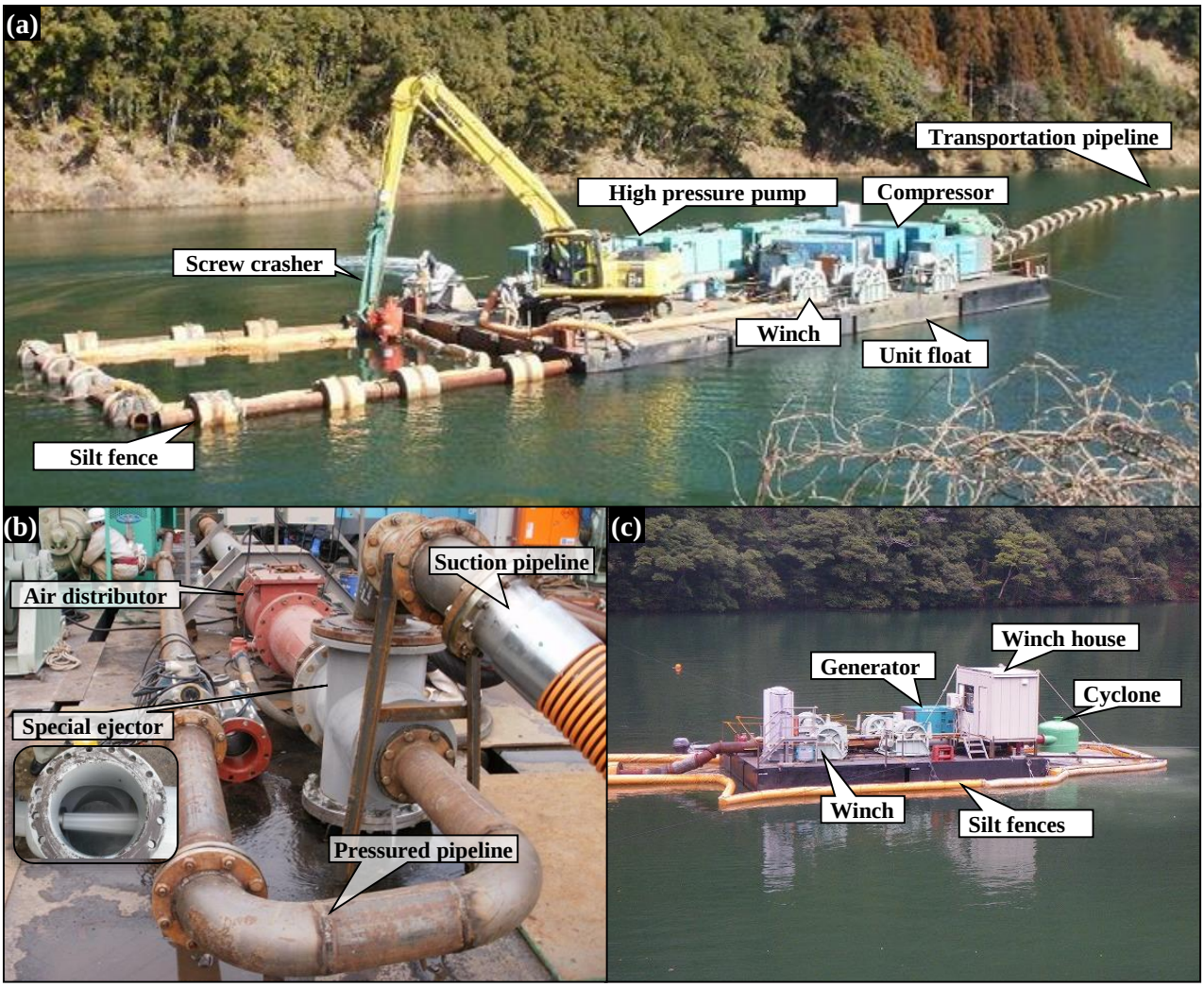

Fig. 11. Field EPDS dredging system: (a) dredging ship; (b) suction system; (c) distributor

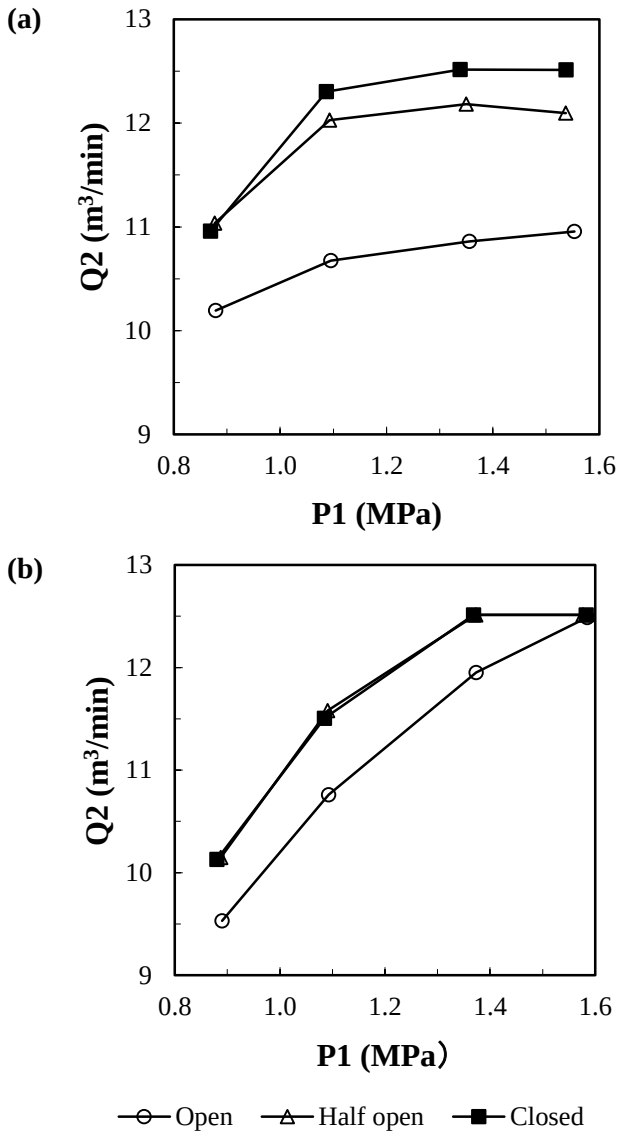

Fig. 12. Flow rate in suction pipe versus average pump pressure for the ejector inner pipe diameters of: (a) 200 mm; (b) 250 mm.

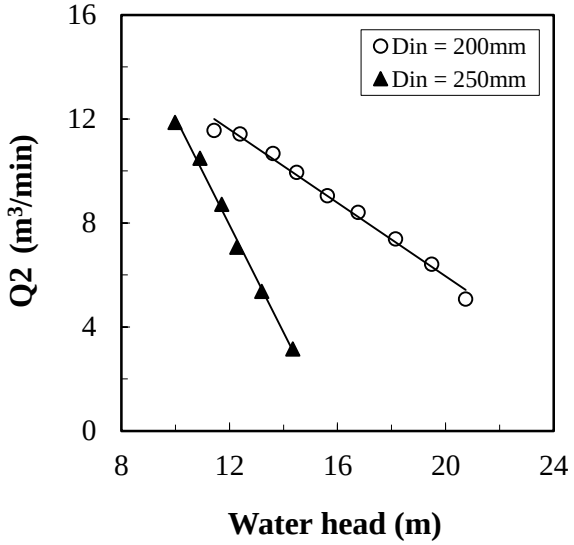

Fig. 13. Relation between suction flow rate (Q2) and water head for different ejector inner diameters.

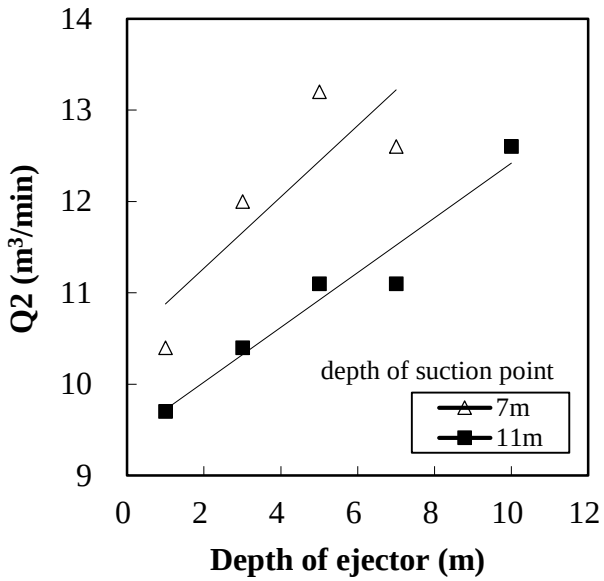

Fig. 14. Suction flow rate (Q2) vs. depth of ejector below water surface using a pump pressure of 1.86 MPa and a 15-m suction pipe

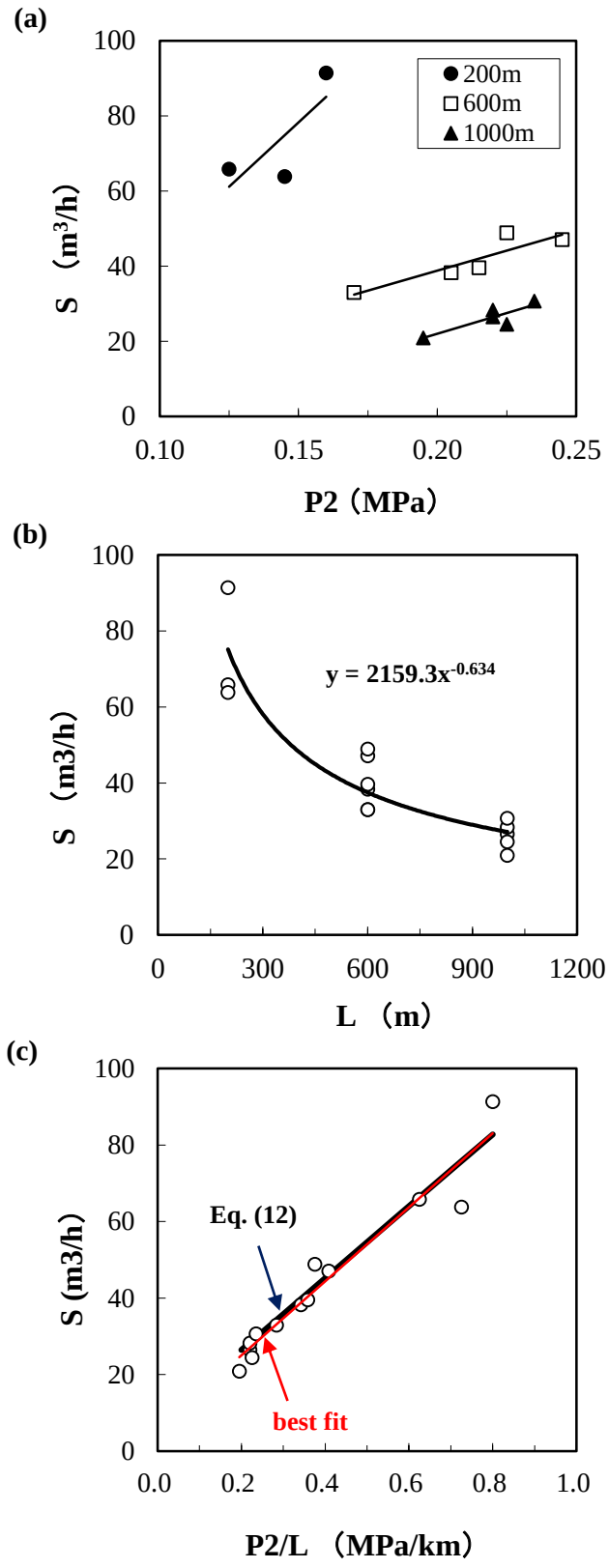

Fig. 15. Sediment transportation rate (S) using EPDS-hopper type for three transport pipe lengths (600, 800, 1000 m): (a) vs P2; (b) vs L; (c) vs. P2/L.

P2 and T: measured and estimated pressure at the starting point of the transport pipe; L: transport pipe length. (Best fit line: $S = 96.8\frac{P2}{L} + 5.7$; Eq. (12): $S = 93.8\frac{T}{L_{tp}} + 7.71$)

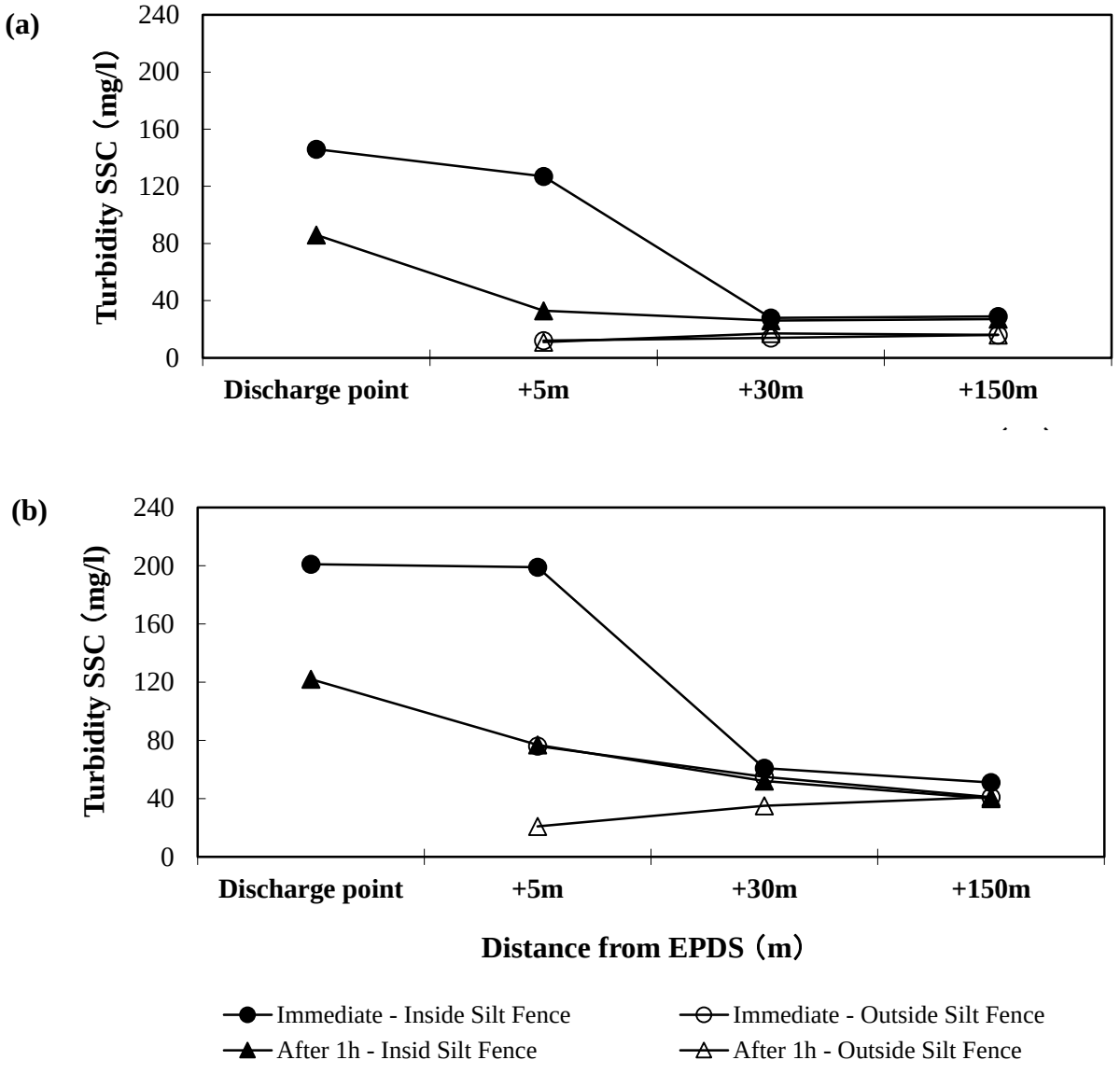

Fig. 16. Turbidity measurements at the vicinity of the EPDS injection points at: (a) water surface; (b) 5 m below the water surface

Table 1 Geometrical and hydraulic parameters for laboratory investigation

Parameter	Range/Value
d_s (mm)	0 (clear), 2, 5, 10, 15 (large), mixed (1:1 bulk volume of 2 and 5 mm)
P_{pump} (kPa)	196, 294, 490, 588, 687
Q_{air} (nl/min)	0, 25, 40, 50, 60, 80, 100, 120
L_{sp} (m)	1, 3, 10, 20
L_{tp} (m)	1, 5, 7, 10, 15, 20, 30
D_{sp} (mm)	25
D_{tp} (mm)	36
H_{suc} (m)	0.2, 1.2, 0.5, 1.5, 2.5

Table 2 EPDS vs commercially available suction dredging systems

System	**Operating**	**Cost** (M ¥)*	**Dredging depth** (m)	**Productivity** (day)*	**Concerns**
EPDS	High pressure pump, jet water	5.85	> 8 m	48	-
Pump dredging	Sand pump with cutter	7.43	> 20 m	51	Turbidity and plugging
Hydro-jet pump	Suction system	2.65	> 50 m	70	Blockage; fine sediment
Siphon dredging	Suction system	2.87	1 – 6 m	39	Clogging
Water injection	Injecting water into bed sediment	3.75	> 14 m	40	Environmental concern; infeasible in consolidated clay silt
Air lift pumps	Pressurized air injection	4.35	> 50 m	30	High water consumption; limited grain size

* per10,000 m^3

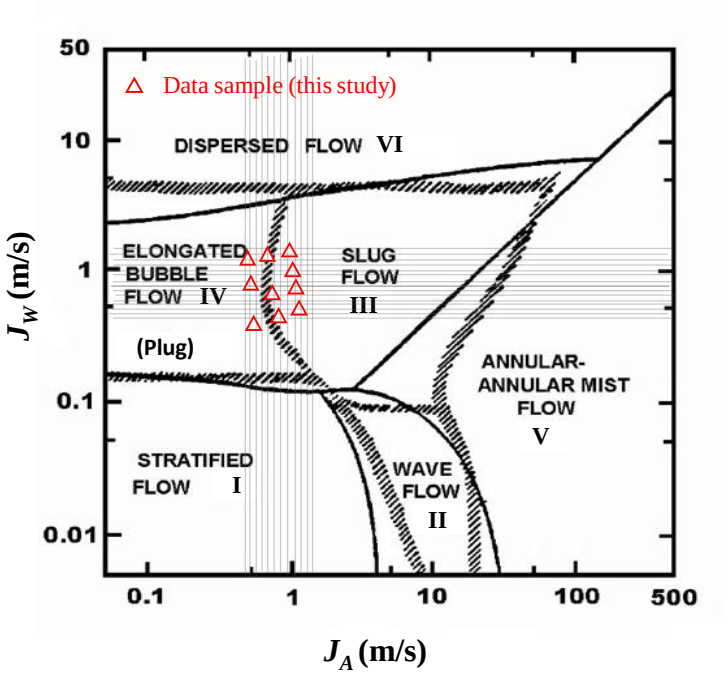

Fig. S1. Superficial velocities of air (J_A) and water (J_w) and flow pattern map in two-phase flow (chart from Mandhane et al.,1974; Taitel and Dukler, 1976);

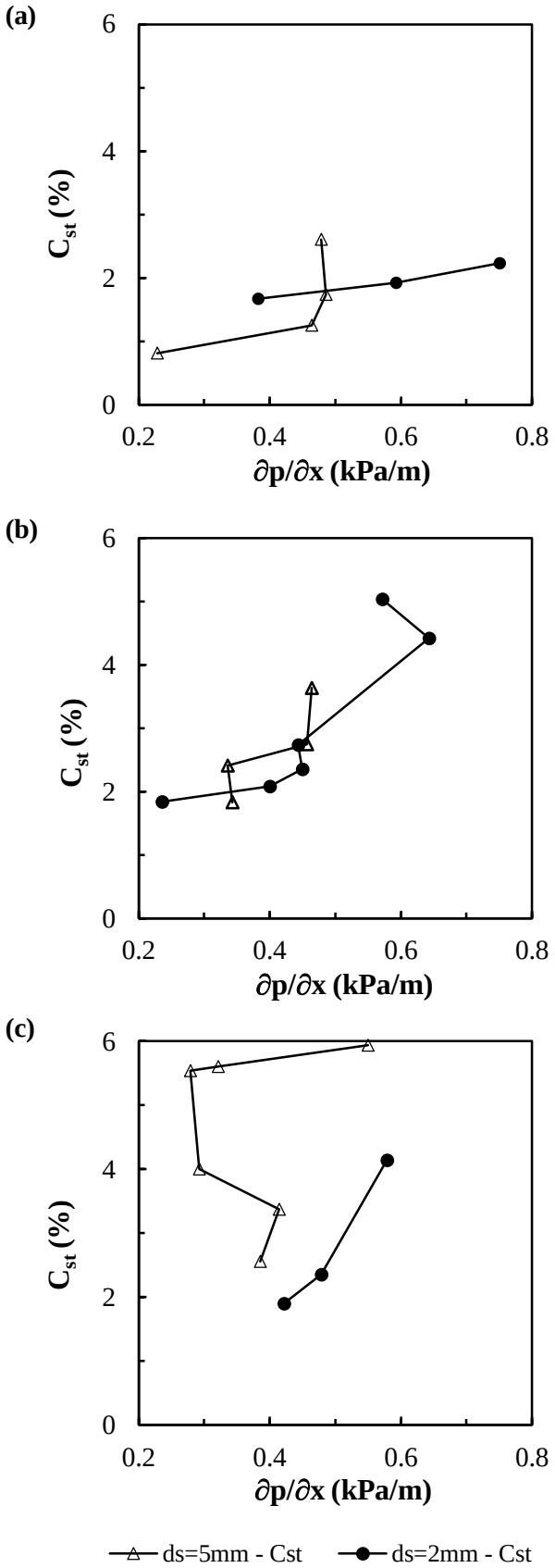

Fig. S2. Sediment removal (C_{st}) vs pressure gradient ($\partial p/\partial x$) for air concentrations of: (a) 0 nl/min; (b) 25 nl/min; (c) 60 nl/min (P_{pump}*=588 kPa*, L_{tp}*= 7 m*).

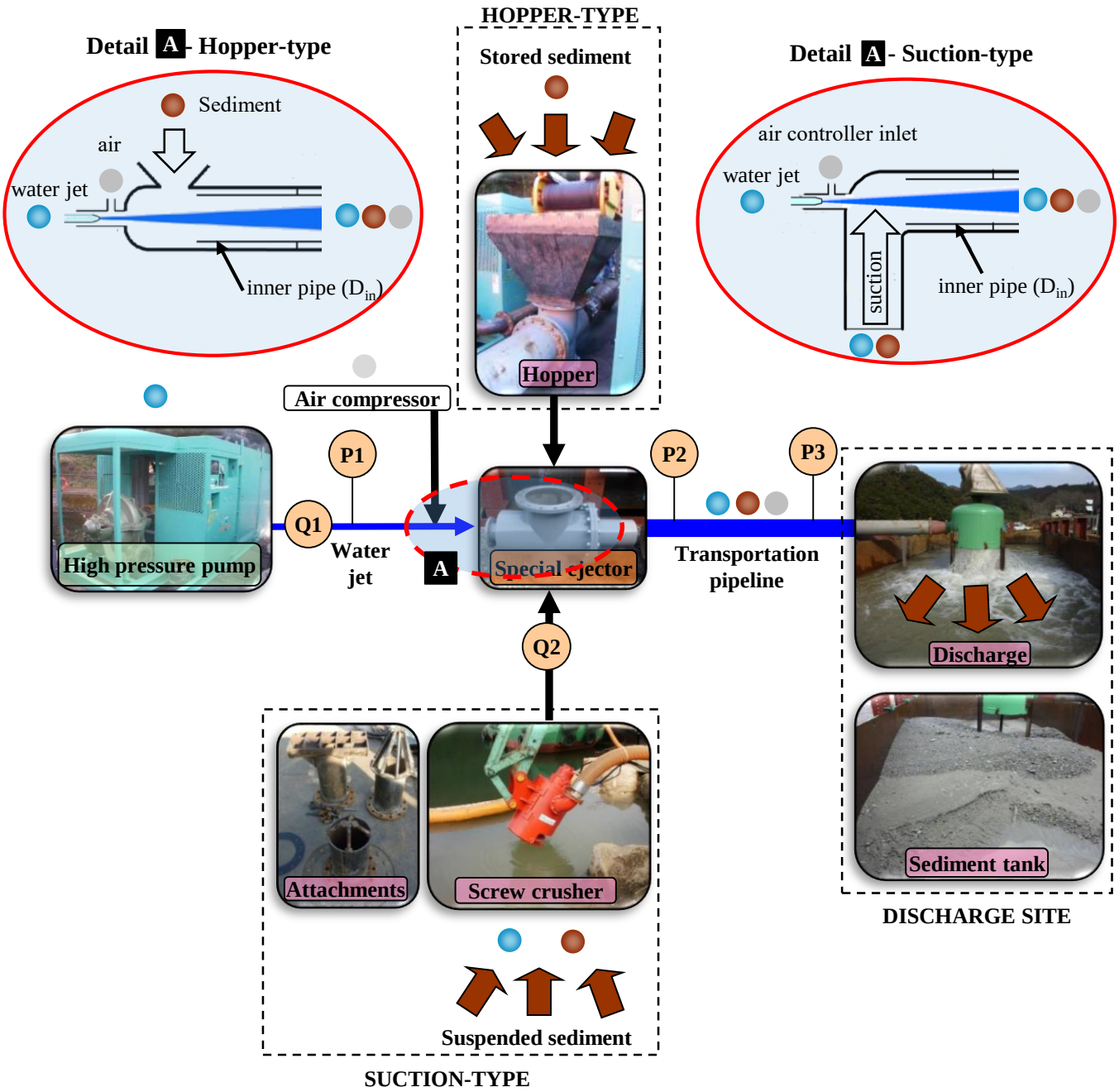

Fig. S3. Sediment dredging system using suction-type and hopper-type EPDS

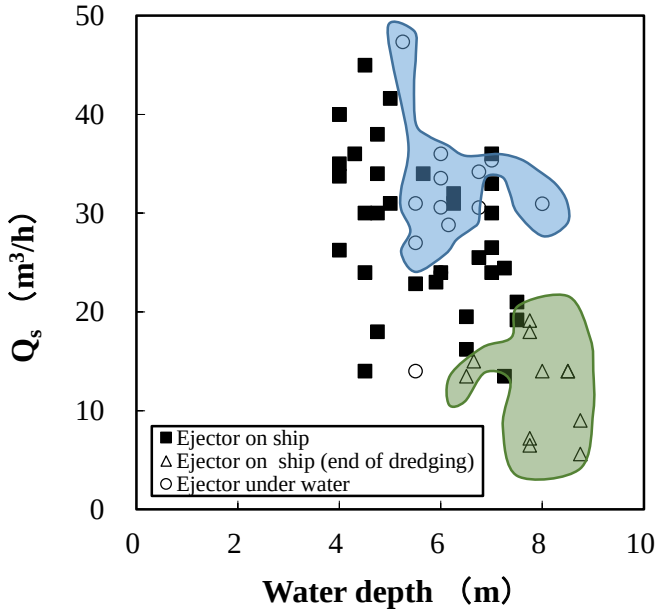

Fig. S4. Water depth and sediment transportation rate through suction (Q_s).

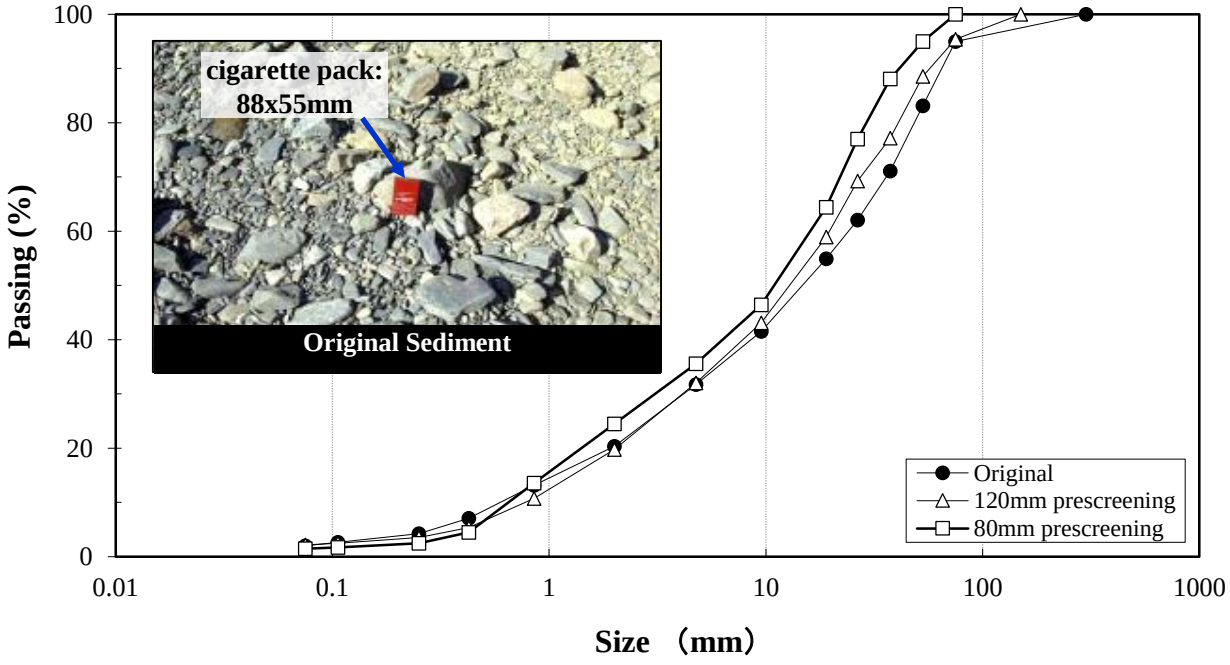

Fig. S5. Grain size distribution of sediments

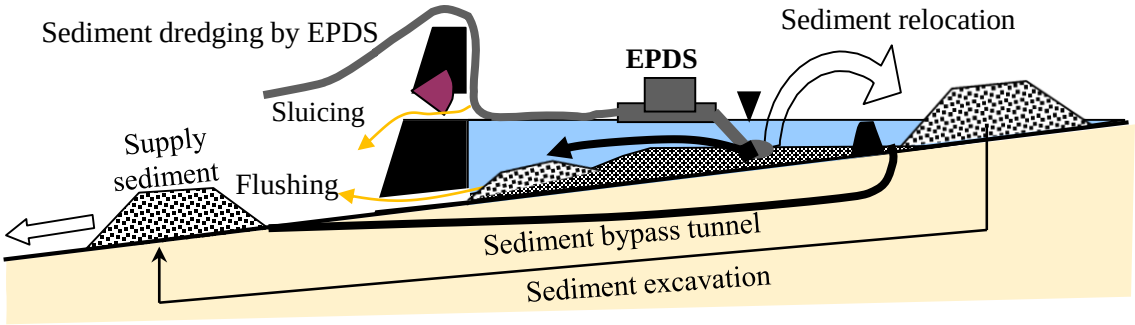

Fig. S6. Utilization of EPS for managing the sediment within the reservoir by relocating, dredging to the downstream, dredging to sediment recycling, and through the spillway. The EPS can be associated with other structures as sediment bypass tunnels and sediment capping for environmental purposes during sluicing.